



TECH BRIEFS

NATIONAL AERONAUTICS AND SPACE ADMINISTRATION

-  **Technology Focus**
-  **Computers/Electronics**
-  **Software**
-  **Materials**
-  **Mechanics**
-  **Machinery/Automation**
-  **Manufacturing**
-  **Bio-Medical**
-  **Physical Sciences**
-  **Information Sciences**
-  **Books and Reports**

INTRODUCTION

Tech Briefs are short announcements of innovations originating from research and development activities of the National Aeronautics and Space Administration. They emphasize information considered likely to be transferable across industrial, regional, or disciplinary lines and are issued to encourage commercial application.

Availability of NASA Tech Briefs and TSPs

Requests for individual Tech Briefs or for Technical Support Packages (TSPs) announced herein should be addressed to

National Technology Transfer Center

Telephone No. (800) 678-6882 or via World Wide Web at www2.nttc.edu/leads/

Please reference the control numbers appearing at the end of each Tech Brief. Information on NASA's Innovative Partnerships Program (IPP), its documents, and services is also available at the same facility or on the World Wide Web at <http://ipp.nasa.gov>.

Innovative Partnerships Offices are located at NASA field centers to provide technology-transfer access to industrial users. Inquiries can be made by contacting NASA field centers and Mission Directorates listed below.

NASA Field Centers and Program Offices

Ames Research Center

Lisa L. Lockyer
(650) 604-1754
lisa.l.lockyer@nasa.gov

Dryden Flight Research Center

Gregory Poteat
(661) 276-3872
greg.poteat@dfrc.nasa.gov

Goddard Space Flight Center

Nona Cheeks
(301) 286-5810
Nona.K.Cheeks.1@nasa.gov

Jet Propulsion Laboratory

Ken Wolfenbarger
(818) 354-3821
james.k.wolfenbarger@jpl.nasa.gov

Johnson Space Center

Helen Lane
(713) 483-7165
helen.w.lane@nasa.gov

Kennedy Space Center

Jim Aliberti
(321) 867-6224
Jim.Aliberti-1@nasa.gov

Langley Research Center

Ray P. Turcotte
(757) 864-8881
r.p.turcotte@larc.nasa.gov

John H. Glenn Research Center at Lewis Field

Robert Lawrence
(216) 433-2921
robert.f.lawrence@nasa.gov

Marshall Space Flight Center

Vernotto McMillan
(256) 544-2615
vernotto.mcmillan@msfc.nasa.gov

Stennis Space Center

John Bailey
(228) 688-1660
john.w.bailey@nasa.gov

NASA Mission Directorates

At NASA Headquarters there are four Mission Directorates under which there are seven major program offices that develop and oversee technology projects of potential interest to industry:

Carl Ray

Small Business Innovation Research Program (SBIR) & Small Business Technology Transfer Program (STTR)
(202) 358-4652
carl.g.ray@nasa.gov

Frank Schowengerdt

Innovative Partnerships Program (Code TD)
(202) 358-2560
fschowen@hq.nasa.gov

John Mankins

Exploration Systems Research and Technology Division
(202) 358-4659
john.c.mankins@nasa.gov

Terry Hertz

Aeronautics and Space Mission Directorate
(202) 358-4636
thertz@mail.hq.nasa.gov

Glen Mucklow

Mission and Systems Management Division (SMD)
(202) 358-2235
gmucklow@mail.hq.nasa.gov

Granville Paules

Mission and Systems Management Division (SMD)
(202) 358-0706
gpaules@mtpe.hq.nasa.gov

Gene Trinh

Human Systems Research and Technology Division (ESMD)
(202) 358-1490
eugene.h.trinh@nasa.gov

John Rush

Space Communications Office (SOMD)
(202) 358-4819
john.j.rush@nasa.gov



TECH BRIEFS

NATIONAL AERONAUTICS AND SPACE ADMINISTRATION



5 Technology Focus: Engineered Materials

- 5 Diamond-Coated Carbon Nanotubes for Efficient Field Emission
- 5 Improved Anode Coatings for Direct Methanol Fuel Cells
- 6 Advanced Ablative Insulators and Methods of Making Them
- 6 PETIs as High-Temperature Resin-Transfer-Molding Materials
- 7 Stable Polyimides for Terrestrial and Space Uses
- 8 Low-Density, Aerogel-Filled Thermal-Insulation Tiles
- 9 High-Performance Polymers Having Low Melt Viscosities
- 10 Nonflammable, Hydrophobic Aerogel Composites for Insulation



11 Electronics/Computers

- 11 Front-Side Microstrip Line Feeding a Raised Antenna Patch
- 12 Medium-Frequency Pseudonoise Georadar



15 Software

- 15 Facilitating Navigation Through Large Archives
- 15 Program for Weibull Analysis of Fatigue Data
- 15 Comprehensive Micromechanics-Analysis Code — Version 4.0
- 15 Component-Based Visualization System
- 16 Software for Engineering Simulations of a Spacecraft
- 16 LabVIEW Interface for PCI-SpaceWire Interface Card
- 16 Path Following With Slip Compensation for a Mars Rover
- 16 International Space Station Electric Power System Performance Code — SPACE
- 17 Software for Automation of Real-Time Agents, Version 2
- 17 Software for Optimizing Plans Involving Interdependent Goals
- 17 Computing Gravitational Fields of Finite-Sized Bodies
- 17 Custom Sky-Image Mosaics From NASA's Information Power Grid

- 18 ANTLR Tree Grammar Generator and Extensions
- 18 Generic Kalman Filter Software



19 Mechanics

- 19 Alignment Stage for a Cryogenic Dilatometer
- 19 Rugged Iris Mechanism



21 Manufacturing

- 21 Treatments To Produce Stabilized Aluminum Mirrors for Cryogenic Uses
- 21 Making AlN_x Tunnel Barriers Using a Low-Energy Nitrogen-Ion Beam
- 22 Making Wide-IF SIS Mixers With Suspended Metal-Beam Leads



25 Physical Sciences

- 25 Sol-Gel Glass Holographic Light-Shaping Diffusers
- 25 Automated Counting of Particles To Quantify Cleanliness
- 26 Phase Correction for GPS Antenna With Nonunique Phase Center
- 27 Compact Infrasonic Windscreen
- 28 Broadband External-Cavity Diode Laser
- 29 High-Efficiency Solar Cells Using Photonic-Bandgap Materials



31 Information Sciences

- 31 Generating Solid Models From Topographical Data
- 31 Computationally Lightweight Air-Traffic-Control Simulation



33 Books & Reports

- 33 Spool Valve for Switching Air Flows Between Two Beds
- 33 Partial Model of Insulator/Insulator Contact Charging
- 33 Asymmetric Electrostatic Radiation Shielding for Spacecraft
- 33 Reusable Hybrid Propellant Modules for Outer-Space Transport

This document was prepared under the sponsorship of the National Aeronautics and Space Administration. Neither the United States Government nor any person acting on behalf of the United States Government assumes any liability resulting from the use of the information contained in this document, or warrants that such use will be free from privately owned rights.



Diamond-Coated Carbon Nanotubes for Efficient Field Emission

Lyndon B. Johnson Space Center, Houston, Texas

Field-emission cathodes containing arrays of carbon nanotubes coated with diamond or diamondlike carbon (DLC) are undergoing development. Multiwalled carbon nanotubes have been shown to perform well as electron field emitters. The idea underlying the present development is that by coating carbon nanotubes with wide-band-gap materials like diamond or DLC, one could reduce effective work functions, thereby reducing threshold electric-field levels for field emission of electrons and, hence, improving cathode performance. To demonstrate feasibility, experimental cathodes were fabricated by (1) covering metal bases with carbon nanotubes

bound to the bases by an electrically conductive binder and (2) coating the nanotubes, variously, with diamond or DLC by plasma-assisted chemical vapor deposition. In tests, the threshold electric-field levels for emission of electrons were reduced by as much as 40 percent, relative to those of uncoated-nanotube cathodes. Coating with diamond or DLC could also make field emission-cathodes operate more stably by helping to prevent evaporation of carbon from nanotubes in the event of overheating of the cathodes. Cathodes of this type are expected to be useful principally as electron sources for cathode-ray tubes and flat-panel displays.

This work was done by Stevan Dimitrijevic and James C. Withers of Materials and Electrochemical Research Corp. for Johnson Space Center.

In accordance with Public Law 96-517, the contractor has elected to retain title to this invention. Inquiries concerning rights for its commercial use should be addressed to:

Materials and Electrochemical Research Corp.

7960 South Kolb Road

Tucson, AZ 85706

Phone: (520) 574-1980

Fax: (520) 574-1983

E-mail: mercorp@mercorp.com

Refer to MSC-23133, volume and number of this NASA Tech Briefs issue, and the page number.

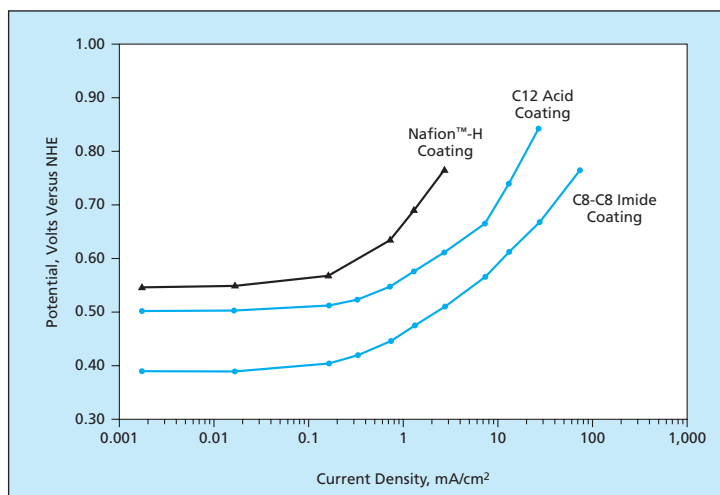
Improved Anode Coatings for Direct Methanol Fuel Cells

Two perfluoroalkanesulfonic compounds offer increased fuel-utilization rates and reduced polarization levels.

NASA's Jet Propulsion Laboratory, Pasadena, California

Two perfluoroalkanesulfonic acids and perfluoroalkanesulfonimides have shown promise as anode-coating materials for improving the performances of direct methanol fuel cells (DMFCs). Heretofore, the state-of-the-art material commonly used for coating anodes in DMFCs has been Nafion™-H — a perfluoro-sulfonic acid-based hydrophilic, proton-conducting ion-exchange polymer that exhibits relatively high thermal and electrochemical stability. Relative to Nafion™-H, the present coating materials afford greater rates of electro-oxidation of methanol, smaller polarization losses and, hence, greater energy-conversion efficiencies.

Perfluorinated solid polymer electrolytes — in particular, Nafion™-H — have been used as anode coatings in



Polarization Levels [potentials versus a normal hydrogen electrode (NHE)] of variously coated carbon-supported Pt-Sn electrodes were measured over a range of current densities in a test cell containing a solution of 1.0 M methanol in 0.50 M sulfuric acid.

DMFCs to (1) ensure contact between electrolyte membranes and electrocatalytic anode materials (typically, alloys containing Pt) and (2) help prevent catalysts from being poisoned by adsorption of anions. However, the perform-

ances of electrodes coated by perfluorinated solid polymer electrolytes have not been ideal, especially at room temperature. Consequently, there has been continued interest in developing means of reducing polarization losses and increasing rates of oxidation and efficiencies of utilization of methanol in order to improve the performances and increase the energy-conversion efficiencies of DMFCs.

In preparation for experiments, DMFC anodes made of carbon-supported Pt, Pt-Ru, and Pt-Sn were prepared and coated, variously, with Nafion™-H or six different perfluoroalkanesulfonic materials: perfluorooctanesulfonic acid (C8 acid), perfluorododecanesulfonic acid (C12 acid), perfluoroheptadecanesulfonic acid (C17 acid), bis-perfluoro-*n*-butyl sulfonyl acid

imide, bis-perfluoro-*n*-octylsulfonic acid imide (C8-C8 imide), or perfluoro-*n*-butyl-perfluoro-*n*-octylsulfonic acid imide. The experiments involved electro-oxidation of methanol on each anode installed as one of the electrodes in a three-electrode electrochemical test cells. The performances of the electrodes were characterized by galvanostatic polarization measurements and cyclic voltammetry. Of the compounds investigated, C12 acid and C8-C8 imide were found to afford the greatest increases in rates of ox-

idation of methanol and the greatest reductions in levels of polarization (see figure), relative to those of Nafion™-H.

This work was done by G. K. Surya Prakash, Qun-jie Wang, and George A. Olah of the University of Southern California and Marshall C. Smart, Sekharipuram Narayanan, and Subbarao Surampudi, of Caltech for NASA's Jet Propulsion Laboratory. Further information is contained in a TSP (see page 1).

In accordance with Public Law 96-517, the contractor has elected to retain title to this

invention. Inquiries concerning rights for its commercial use should be addressed to:

*Innovative Technology Assets Management
JPL*

*Mail Stop 202-233
4800 Oak Grove Drive
Pasadena, CA 91109-8099
(818) 354-2240*

E-mail: iaoffice@jpl.nasa.gov

Refer to NPO-40503, volume and number of this NASA Tech Briefs issue, and the page number

Advanced Ablative Insulators and Methods of Making Them Reinforced, filled silicones and carbon phenolics are laser-milled to final shapes.

Lyndon B. Johnson Space Center, Houston, Texas

Advanced ablative (more specifically, charring) materials that provide temporary protection against high temperatures, and advanced methods of designing and manufacturing insulators based on these materials, are undergoing development. These materials and methods were conceived in an effort to replace the traditional thermal-protection systems (TPSs) of re-entry spacecraft with robust, lightweight, better-performing TPSs that can be designed and manufactured more rapidly and at lower cost. These materials and methods could also be used to make improved TPSs for general aerospace, military, and industrial applications.

The ablative materials belong to two families. One family comprises filled,

fiber-reinforced elastomeric carbon phenolics with mass densities that range from 18 to 40 lbm/ft³ (288 to 641 kg/m³); these materials are designed to protect against heating rates up to about 1,300 Btu/(ft²s) [\approx 15 MW/m²]. The other family comprises filled, fiber-reinforced silicones with mass densities that range from 12 to 50 lbm/ft³ [192 to 800 kg/m³]; these materials are designed to protect against heating rates from 5 to about 400 Btu/(ft²s) [about 0.06 to about 4.5 MW/m²]. The fillers in these materials help to minimize their mass densities, while the fibers help to maximize their strengths.

Design and manufacture of TPSs according to the present approach involve the use of computer-aided design

and computer-aided manufacturing (CAD/CAM) methods, including computer numerically controlled (CNC) laser milling. This approach eliminates the labor-intensive steps of machining, fitting, and trimming heat-shield parts in the prior approach to manufacturing. In the present approach, molded panels of the ablative materials are CNC-laser-milled to precise final sizes and shapes and are thus made ready for bonding to heat-shield structures.

This work was done by William M. Congdon of Applied Research Associates, Inc., for Johnson Space Center. For further information, contact the Johnson Technology Transfer Office at (281) 483-3809. MSC-23141

PETIs as High-Temperature Resin-Transfer-Molding Materials PETI-matrix/carbon-fiber composites made by resin-transfer molding have excellent properties.

Langley Research Center, Hampton, Virginia

Compositions of, and processes for fabricating, high-temperature composite materials from phenylethynyl-terminated imide (PETI) oligomers by resin-transfer molding (RTM) and resin infusion have been developed. Composites having a combination of excellent mechanical properties and long-term high-temperature stability have been readily fabricated. These materials are particularly useful for the fabrication of high-temperature structures for jet-engine components, structural components on high-speed aircraft, spacecraft, and missiles.

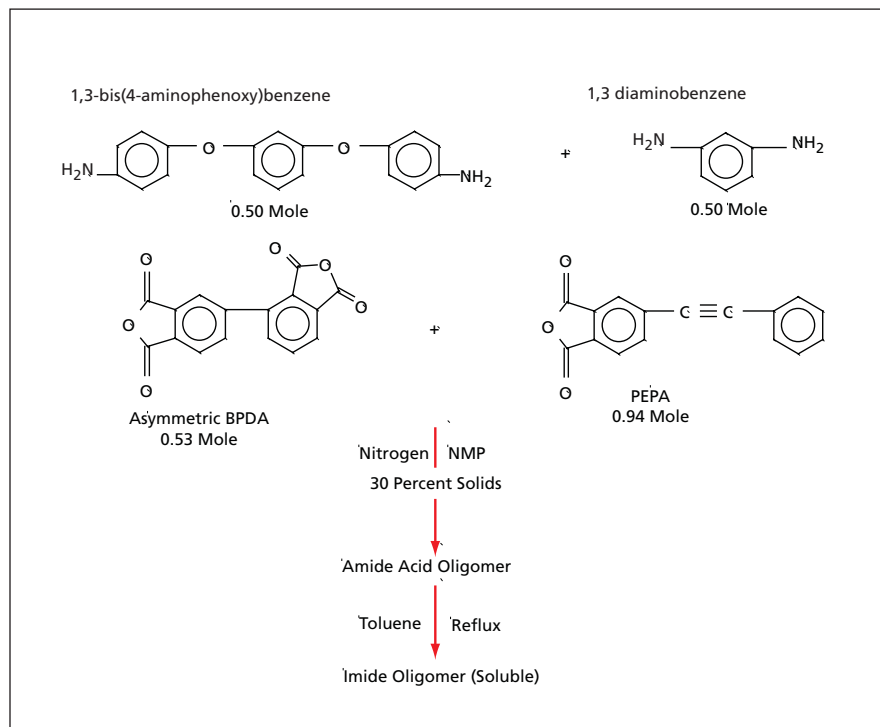
Phenylethynyl-terminated amide acid oligomers that are precursors of PETI oligomers are easily made through the reaction of a mixture of aromatic diamines with aromatic dianhydrides at high stoichiometric offsets and 4-phenylethynylphthalic anhydride (PEPA) as an end-capper in a polar solvent such as *N*-methylpyrrolidinone (NMP). These oligomers are subsequently cyclodehydrated — for example, by heating the solution in the presence of toluene to remove the water by azeotropic distillation to form low-molecular-weight imide

oligomers. More precisely, what is obtained is a mixture of PETI oligomeric species, spanning a range of molecular weights, that exhibits a stable melt viscosity of less than approximately 60 poise (and generally less than 10 poise) at a temperature below 300 °C. After curing of the oligomers at a temperature of 371 °C, the resulting polymer can have a glass-transition temperature (T_g) as high as 375 °C, the exact value depending on the compositions.

As an example, one PETI oligomer, denoted PETI-330, was synthesized as

shown in the figure. First, 0.53 mole of 2,3,3',4'-biphenyltetracarboxylic dianhydride (BPDA) and 0.94 mole of PEPA were reacted with 0.50 mole of 1,3-bis(4-aminophenoxy)benzene and 0.50 mole of 1,3-diaminobenzene in NMP to form the phenylethynyl-terminated amide acid oligomer. Then, by azeotropic distillation using toluene, the phenylethynyl-terminated amide acid oligomer was converted to the PETI oligomer having a calculated repeat unit molecular weight of 750 g/mole. The imide oligomer was isolated, washed well with water, and dried. The melt viscosity of the imide oligomer was found to be 0.6 poise initially at a temperature of 280 °C and 0.9 poise after 2 hours at that temperature.

The imide oligomer was degassed, then injected, at a temperature of 280 °C, into a preform made of a fabric of T650 carbon fibers in 8-harness satin weave. The oligomer was then cured for 1 hour at a temperature of 371 °C and a pressure of 200 psi (≈ 1.4 MPa). The resulting quasi-isotropic composite was found to have an open-hole compressive strength of 39 kpsi (≈ 0.27 GPa) at a temperature of 23 °C and 29 kpsi (≈ 0.2 GPa) at a temperature of 288 °C. After aging for 1,000 hours at 288 °C in air, the open-hole compressive strength was found to be 32 kpsi (≈ 0.22 GPa) at 23 °C. The unnotched compressive strength was found to be 75 kpsi (≈ 0.52 GPa) at 23 °C. The composite exhibited no microcracking, either



PETI-330 is Synthesized in this sequence of reactions.

immediately after cure or after 200 subsequent thermal cycles from -55 °C to $+288$ °C. The T_g of the composite was found to be 330 °C.

Another such PETI oligomer, denoted PETI-375, was synthesized and used to make an RTM composite with a carbon-fiber cloth of the type described above. The open-hole compressive strength of this composite was found to be 43.5 kpsi

(≈ 0.3 GPa) at 23 °C, 34.8 kpsi (≈ 0.24 GPa) at 288 °C, and 32.2 kpsi (≈ 0.22 GPa) at 316 °C. The T_g of the composite was found to be 370 °C.

This work was done by John W. Connell, Joseph G. Smith, Jr., and Paul M. Hergenrother of Langley Research Center. Further information is contained in a TSP (see page 1). LAR-15834-1

Stable Polyimides for Terrestrial and Space Uses

Low-color films exhibit high resistance to space environment.

Langley Research Center, Hampton, Virginia

Polyimides of a recently developed type have an attractive combination of properties, including low solar absorptivity (manifested as low color) when cast into thin films, resistance to atomic oxygen and ultraviolet radiation, solubility in organic solvents, high glass-transition temperatures (T_g s), and high thermal stability. The focus of the development work was on polymers that can endure the space environment and that have specific combinations of properties for use on Gossamer spacecraft. Because of their unique combination of properties, these polymers are also expected to find use in a variety of other applications on Earth as well as in space.

Examples of other space applications include membranes on antennas, second-surface mirrors, thermal optical coatings, and multilayer thermal insulation. For both terrestrial and space applications, these polyimides can be processed into various forms, including films, fibers, foams, threads, adhesives, and coatings.

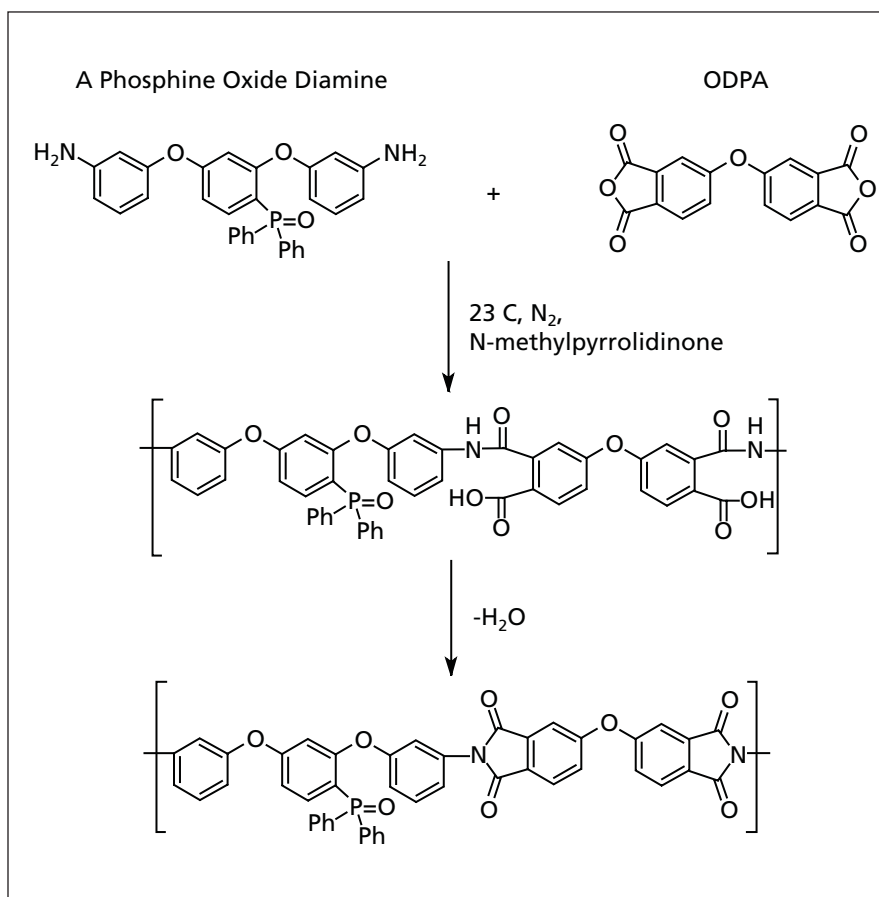
In preparation for synthesizing a polyimide of this type, one makes [2,4-bis(3-aminophenoxy)phenyl]diphosphine oxide (hereafter denoted "the phosphine oxide diamine"), which is a novel aromatic diamine. In an experiment, this aromatic diamine was made from commercially available starting ma-

terials in a two-step process in relatively high yield. Then, in experimental syntheses of polyimides of this type, the phosphine oxide diamine was reacted with aromatic dianhydrides in polar aprotic solvents. In other experiments, copolyimides were synthesized by use of the phosphine oxide diamine in combination with other commercially available aromatic diamines. These various syntheses made it possible to tailor the polymers to reduce costs and obtain hitherto unavailable combinations of properties.

The figure illustrates the example of one synthesis, in which the phosphine oxide diamine was reacted with oxydiphthalic anhydride (ODPA) in N-methyl-

pyrrolidinone (a polar aprotic solvent) at 20 weight percent to form a polyamide acid having an inherent viscosity of 1.01 dL/g. The polyamide acid was converted to the polyimide by reaction with a mixture of acetic anhydride and pyridine. The polyimide was isolated, dried, and dissolved in N,N-dimethylacetamide, then thin films were cast and stage-dried at temperatures up to 250 °C for one hour. A 1.6-mil (≈ 0.04 -mm)-thick film was found to have 85-percent transparency at a wavelength of 500 nm, solar absorptivity of 0.06, thermal emissivity of 0.56, T_g of 212 °C, 5-percent loss of weight upon heating in air at a rate of 2.5 °C/minute up to 461 °C, and the following tensile properties at a temperature of 23 °C: strength of 14.7 kpsi (≈ 101 MPa), modulus of 410 kpsi (≈ 2.8 GPa), and elongation of 4.7 percent. A film subjected to atomic oxygen in a ground-based experiment that simulated 6 months in a low orbit around the Earth exhibited 81-percent transmission at 500 nm, only 1.74-percent of mass loss, and excellent retention of properties in general.

In another example, a copolyimide was made from the reaction of ODPA with 75 mole percent of the phosphine oxide diamine and 25 mole percent of 3,4'-oxydianiline. A 1-mil (≈ 0.025 -mm)-thick film of this copolyimide was found to have 88-percent transparency at a wavelength of 500 nm, solar absorptivity of 0.06, thermal emissivity of 0.38, T_g of 218 °C, and the following tensile properties at a temperature of 23 °C: strength of 14.7 kpsi (≈ 101 MPa), modulus of 460 kpsi (≈ 3.2 GPa), and elongation of 6.3 percent.



A Phosphine Oxide Diamine Was Reacted With ODPA to obtain a polyimide that strongly resists degradation under space conditions.

This work was done by John W. Connell, Joseph G. Smith, Jr., and Paul M. Hergenrother of Langley Research Center, and Kent A. Watson and Craig M. Thompson of the National Institute of Aerospace. The technology is covered in Patent Application No. US

2003/0045670 A1 and NASA Case No. LAR 16176-1 and was exclusively licensed to Triton Systems, Inc. Requests for information on this technology should be directed to Norm Rice at nrice@tritonsys.com. LAR-16176-1

Low-Density, Aerogel-Filled Thermal-Insulation Tiles

Lyndon B. Johnson Space Center, Houston, Texas

Aerogel fillings have been investigated in a continuing effort to develop low-density thermal-insulation tiles that, relative to prior such tiles, have greater dimensional stability (especially less shrinkage), equal or lower thermal conductivity, and greater strength and durability. In preparation for laboratory tests of dimensional and thermal stability, prototypes of aerogel-filled versions of recently developed low-density tiles have been fabricated by impregnating such tiles to various depths with aerogel formations ranging in density from 1.5 to 5.6 lb/ft³ (about 53 to 200 kg/m³). Results available at the time of report-

ing the information for this article showed that the thermal-insulation properties of the partially or fully aerogel-impregnated tiles were equivalent or superior to those of the corresponding non-impregnated tiles and that the partially impregnated tiles exhibited minimal (<1.5 percent) shrinkage after multiple exposures at a temperature of 2,300 °F (1,260 °C). Latest developments have shown that tiles containing aerogels at the higher end of the density range are stable after multiple exposures at the said temperature.

This work was done by Maryann Santos, Vann Heng, Alfred Zinn, Andrea Barney,

Kris Oka, and Michael Droege of the Boeing Co. for Johnson Space Center. For further information, contact the Johnson Technology Transfer Office at (281) 483-3809.

Title to this invention has been waived under the provisions of the National Aeronautics and Space Act {42 U.S.C. 2457(f)} to The Boeing Company. Inquiries concerning licenses for its commercial development should be addressed to:

*Boeing Company
5301 Bolsa Ave.*

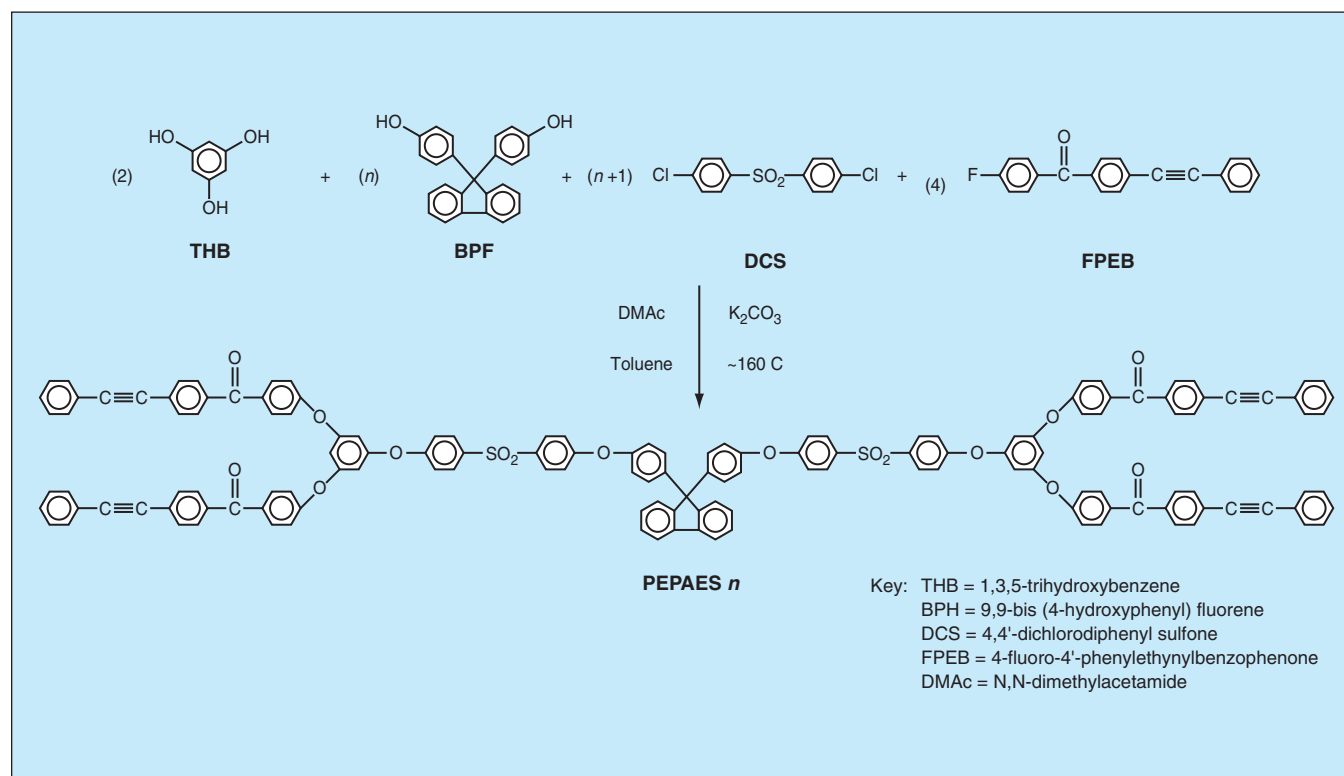
Huntington Beach, CA 92657-2099

Refer to MSC-23393, volume and number of this NASA Tech Briefs issue, and the page number.

High-Performance Polymers Having Low Melt Viscosities

Mixtures of differently shaped molecules have properties superior to the corresponding linear polymers.

Langley Research Center, Hampton, Virginia



A Phenylethynyl Poly(Arylene Ether) Sulfone (PEPAES) or, more accurately, a mixture of PEPAES molecules having different values of the integer n , is synthesized according to this reaction scheme.

High-performance polymers that have improved processing characteristics, and a method of making them, have been invented. One of the improved characteristics is low (relative to corresponding prior polymers) melt viscosities at given temperatures. This characteristic makes it possible to utilize such processes as resin-transfer molding and resin-film infusion and to perform autoclave processing at lower temperatures and/or pressures. Another improved characteristic is larger processing windows — that is, longer times at low viscosities. Other improved characteristics include increased solubility of uncured polymer precursors that contain reactive groups, greater densities of cross-links in cured polymers, improved mechanical properties of the cured polymers, and greater resistance of the cured polymers to chemical attack.

The invention is particularly applicable to poly(arylene ether)s [PAEs] and polyimides [PIs] that are useful as adhesives, matrices of composite materi-

als, moldings, films, and coatings. PAEs and PIs synthesized according to the invention comprise mixtures of branched, linear, and star-shaped molecules. The monomers of these polymers can be capped with either reactive end groups to obtain thermosets or nonreactive end groups to obtain thermoplastics. The synthesis of a polymeric mixture according to the invention involves the use of a small amount of a trifunctional monomer. In the case of a PAE, the trifunctional monomer is a trihydroxy-containing compound — for example, 1,3,5-trihydroxybenzene (THB). In the case of a PI, the trifunctional monomer is a triamine — for example, triamino pyrimidine or melamine. In addition to the aforementioned trifunctional monomer, one uses the difunctional monomers of the conventional formulation of the polymer in question (see figure).

In cases of nonreactive end caps, the polymeric mixtures of the invention have melt viscosities and melting temperatures lower than those of the corre-

sponding linear polymers of equal molecular weights. The lower melting temperatures and melt viscosities provide larger processing windows.

In cases of reactive end caps, the polymeric mixtures of the invention have lower melt viscosities before curing and the higher cross-link densities after curing (where branching in the uncured systems would become cross-links in the cured systems), relative to the corresponding linear polymers of equal molecular weights. The greater cross-link densities afford increased resistance to chemical attack and improved mechanical properties.

This work was done by Brian J. Jensen of Langley Research Center. Further information is contained in a TSP (see page 1).

This invention has been patented by NASA (U.S. Patent Nos. 5,965,687 and 6,191,252). Inquiries concerning nonexclusive or exclusive license for its commercial development should be addressed to the Patent Counsel, Langley Research Center, at (757) 864-3521. Refer to LAR-15534.

Nonflammable, Hydrophobic Aerogel Composites for Insulation

Lyndon B. Johnson Space Center, Houston, Texas

Aerogel composites that are both nonflammable and hydrophobic have been developed for use as lightweight thermal-insulation materials for cryogenic systems. Aerogels are well known in the industry for their effectiveness as thermal insulators under cryogenic conditions, but the treatments used heretofore to render them hydrophobic also make them flammable. Nonflammability would make it safer to use aerogel insulation, especially in oxygen-rich environments and on cryogenic systems that contain liquid oxygen.

A composite of this type is a silica aerogel reinforced with fibers. In comparison with unreinforced aerogels, the aerogel composite is about ten times as stiff and strong, better able to withstand handling, and more amenable to machining to required shapes. The composite can be made hydrophobic and nonflammable by appropriate design of a sol-gel process used to synthesize the aerogel component.

In addition to very low thermal conductivity needed for insulation, aerogel composites of this type have been found

to exhibit high resistance to moisture and nonflammability in oxygen-rich atmospheres: Samples floating on water for months gained no weight and showed no signs of deterioration. Samples were found to be nonflammable, even in pure oxygen at atmospheric pressure [14.7 psia (0.10 MPa)].

*This work was done by Begag Redouane of Aspen Systems, Inc., for **Johnson Space Center**. For further information, contact the Johnson Technology Transfer Office at (281) 483-3809.
MSC-23265*



Front-Side Microstrip Line Feeding a Raised Antenna Patch

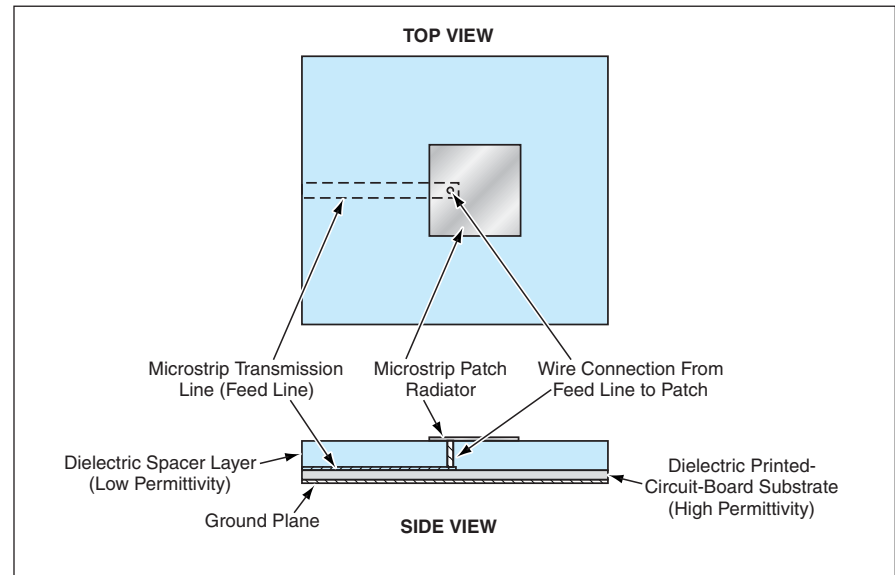
Relative to prior patch antennas, this is simpler, thinner, and less expensive.

NASA's Jet Propulsion Laboratory, Pasadena, California

An improved design concept for a printed-circuit patch antenna and the transmission line that feeds the patch calls for (1) a microstrip transmission line on the front (radiative) side of a printed-circuit board based on a thin, high-permittivity dielectric substrate; (2) using the conductor covering the back side of the circuit board as a common ground plane for both the microstrip line and the antenna patch; (3) supporting the antenna patch in front of the circuit board on a much thicker, lower-permittivity dielectric spacer layer; and (4) connecting the microstrip transmission line to the patch by use of a thin wire or narrow ribbon that extends through the thickness of the spacer and is oriented perpendicularly to the circuit-board plane. The thickness of the substrate is typically chosen so that a microstrip transmission line of practical width has an impedance between 50 and 100 Ω . The advantages of this design concept are best understood in the context of the disadvantages of prior design concepts, as explained below.

One prior design concept involves the use of a probe feed, in which the coupling between a transmission line behind the ground plane and an antenna patch on the front side of the circuit board is effected by a small wire that passes through a coaxial hole in the ground plane and the printed-circuit-board substrate. In another prior design concept, a transmission line on the back and an antenna patch on the front are coupled magnetically via slots. In yet another prior design concept, the antenna patch and its microstrip feed line are both formed on the front surface of the printed-circuit board along with the rest of the printed circuitry.

Probe- and slot-coupling designs exhibit a tendency toward leakage of radiation from the transmission-line region behind the antenna. Leakage can be reduced by shielding the microstrip or making it asymmetrical, but this undesirably increases the thickness of the antenna and causes excitation of parallel-plate modes that have a zero cutoff frequency, contribute spikes to the re-



This Relatively Simple Patch Antenna performs as well as or better than does a more complex and expensive prior patch antenna.

turn-loss spectrum, and sometimes make the antenna “blind” in some directions. Special mode-suppression pins, or vias, can be used in probe coupling to suppress the parallel-plate modes, but this significantly increases the cost, complexity, and size of the antenna. In addition, fabrication of the feed line at the thickness and permittivity that optimize connection to the patch antenna tends to make coupling to the next layer behind the feed circuit very difficult.

The prior design concept in which the microstrip feed is printed on the same surface as that of the antenna patch is seldom implemented and is fraught with drawbacks. First, the thickness and permittivity needed for a microstrip transmission line tend to result in a very narrow-band and inefficient microstrip radiator. To increase the radiative bandwidth of the patch, one must increase the substrate thickness, but this increases the percentage of power launched into the lowest order transverse magnetic surface wave mode, resulting in greatly reduced efficiency and loss of control over the radiation pattern. A second drawback is that the patch takes up so much space on the circuit board that there is very little area

available for placement of feed lines. The only alternative is to place the feed lines close together and close to the patch, leading to undesired cross coupling between lines and patches, scattering of radiation, and consequent loss of control of the radiation pattern.

In the improved design concept, the low-permittivity thick-spacer and direct-connection features, taken together, result in a good impedance match with suppression of unwanted cross-coupling and scattering. By eliminating the feed circuitry from behind the ground plane and eliminating all holes through the ground plane, this design concept eliminates the leakage-suppression problem and, hence, the drawbacks of the leakage-suppression techniques. Moreover, because there is no feed circuitry behind the ground plane, the overall antenna package is much thinner than it would otherwise be. Other advantages of this design concept include the following:

- Any desired additional electronic circuits can be placed behind the ground plane with little or no risk of electromagnetic interference because these circuits are inherently shielded by the ground plane. If it is necessary to make

an electrical connection through the ground plane, a coaxial connector can be optimized to maintain shielding.

- Because the microstrip line and the antenna are printed on different dielectric substrates, the aforementioned limitation on available area no longer applies.
- Also, because the microstrip line and the antenna are printed on different substrates, the substrate for the transmission can be thin and of high relative

permittivity (typically between 2 and 10), as needed for a low-leakage transmission line, while the antenna patch can be printed on a thick, low-relative-permittivity substrate to maximize bandwidth and suppress surface waves.

This work was done by Richard Hodges and Daniel Hoppe of Caltech for NASA's Jet Propulsion Laboratory. Further information is contained in a TSP (see page 1).

In accordance with Public Law 96-517, the contractor has elected to retain title to this

invention. Inquiries concerning rights for its commercial use should be addressed to:

*Innovative Technology Assets Management
JPL*

*Mail Stop 202-233
4800 Oak Grove Drive
Pasadena, CA 91109-8099
(818) 354-2240*

*E-mail: iaoffice@jpl.nasa.gov
Refer to NPO-30605, volume and number of this NASA Tech Briefs issue, and the page number.*

Medium-Frequency Pseudonoise Georadar

It would not be necessary to trade away resolution against penetration distance.

Lyndon B. Johnson Space Center, Houston, Texas

Ground-probing radar systems featuring medium-frequency carrier signals phase-modulated by binary pseudonoise codes have been proposed. These systems would be used to locate and detect movements of subterranean surfaces; the primary intended application is in warning of the movement of underground water toward oil-well intake ports in time to shut down those ports to avoid pumping of water. Other potential applications include oil-well logging and monitoring of un-

derground reservoirs.

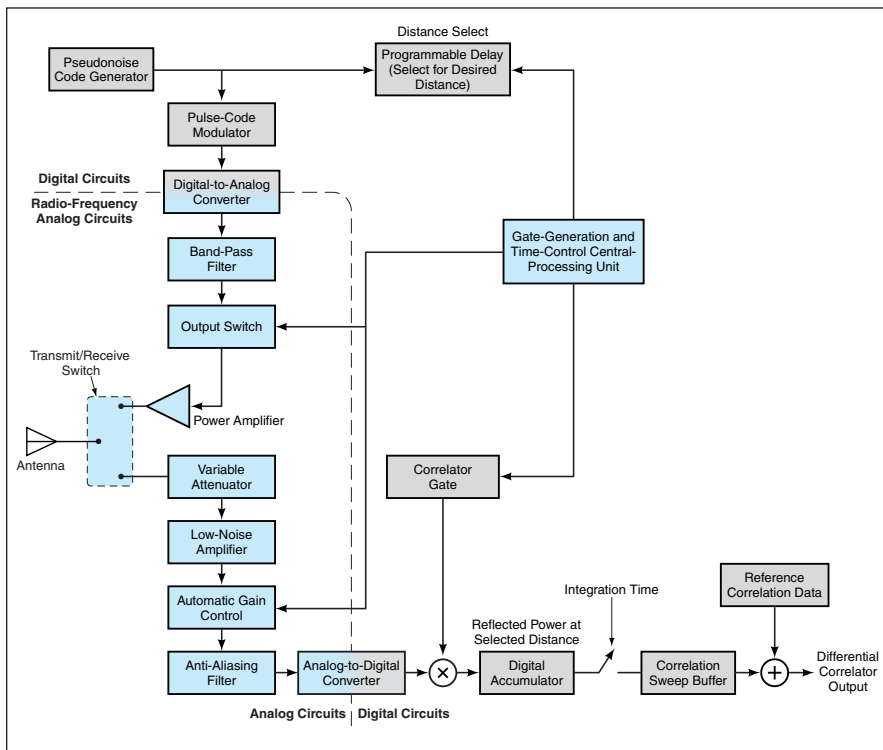
A typical prior georadar system operates at a carrier frequency of at least 50 MHz in order to provide useable range resolution. This frequency is too high for adequate penetration of many underground layers of interest. On the other hand, if the carrier frequency were to be reduced greatly to increase penetration, then bandwidth and thus range resolution would also have to be reduced, thereby rendering the system less useful. The proposed medium-fre-

quency pseudonoise georadar systems would offer the advantage of greater penetration at lower carrier frequencies, but without the loss of resolution that would be incurred by operating typical prior georadar systems at lower frequencies.

The figure is a block diagram of a system according to the proposal. The transmitter would operate at a carrier frequency chosen primarily according to the electrical conductivity and permittivity of the underground region of interest; ordinarily, one would use a frequency < 1 MHz in a high-conductivity region or > 1 MHz in a low-conductivity region. The carrier signal would be phase-modulated with pseudonoise pulses representing "0" or "1" phase states. Between pseudonoise pulses, the transmitter would be turned off and the receiver turned on to detect reflections. Signal-propagation times, and thus distances to interfaces, would be determined by processing the demodulated received signals with various delays to find correlations between the received signals and the transmitted pseudonoise code.

Propagation of medium-frequency electromagnetic signals in the underground environment involves dispersion and frequency-dependent attenuation, which introduce spectral distortion. The receiver would include filters that would compensate for this distortion.

The time gating of the transmitter and receiver would reduce the probability that the high power and short delay of reflections from nearby interfaces would degrade the response of the receiver to low-power reflections from dis-



A Medium-Frequency Pseudonoise Georadar System would contain a combination of digital signal-generating and -processing circuits and analog radio-frequency transmitting and receiving circuits to implement a pseudonoise ranging technique for locating underground water fronts and possibly other interfaces.

tant interfaces. A further contribution to the needed dynamic range would be made by automatic gain control and/or an electronically controlled variable attenuator.

Much of the system would be digital. The system could be configured digitally to function in a wide variety of geological formations that may be encountered at depths from zero to thousands

of meters. For example, the length of the pseudonoise code could be chosen according to how much processing gain is needed to extract the desired return signal from the noise-corrupted received signal. A longer code entails longer detection time. Because of the slowness of motion of underground water fronts, there is usually sufficient time for processing a long code.

*This work was done by G. Dickey Arndt of **Johnson Space Center**, J. R. Carl of Lockheed Martin, Kent A. Byerly of Spacial Acuity Co., and B. Jon Amini of Winn Fuel Systems.*

This invention is owned by NASA, and a patent application has been filed. Inquiries concerning nonexclusive or exclusive license for its commercial development should be addressed to the Patent Counsel, Johnson Space Center, (281) 483-0837. Refer to MSC-23029.

Facilitating Navigation Through Large Archives

Automated Visual Access (AVA) is a computer program that effectively makes a large collection of information visible in a manner that enables a user to quickly and efficiently locate information resources, with minimal need for conventional keyword searches and perusal of complex hierarchical directory systems. AVA includes three key components: (1) a taxonomy that comprises a collection of words and phrases, clustered according to meaning, that are used to classify information resources; (2) a statistical indexing and scoring engine; and (3) a component that generates a graphical user interface that uses the scoring data to generate a visual map of resources and topics. The top level of an AVA display is a pictorial representation of an information archive. The user enters the depicted archive by either clicking on a depiction of subject area cluster, selecting a topic from a list, or entering a query into a text box. The resulting display enables the user to view candidate information entities at various levels of detail. Resources are grouped spatially by topic with greatest generality at the top layer and increasing detail with depth. The user can zoom in or out of specific sites or into greater or lesser content detail.

This program was written by Robert O. Shelton of Johnson Space Center, Stephanie L. Smith of LinCom, and Dat Truong and Terry R. Hodgson of Science Applications International Corp.

The code is copyrighted and is available for licensing. For further information, contact the Johnson Technology Transfer Office at (281) 483-3809. MSC-23542

Program for Weibull Analysis of Fatigue Data

A Fortran computer program has been written for performing statistical analyses of fatigue-test data that are assumed to be adequately represented by a two-parameter Weibull distribution. This program calculates the following:

- Maximum-likelihood estimates of the Weibull distribution;
- Data for contour plots of relative likelihood for two parameters;
- Data for contour plots of joint confidence regions;
- Data for the profile likelihood of the Weibull-distribution parameters;

- Data for the profile likelihood of any percentile of the distribution; and
- Likelihood-based confidence intervals for parameters and/or percentiles of the distribution.

The program can account for tests that are suspended without failure (the statistical term for such suspension of tests is “censoring”). The analytical approach followed in this program for the software is valid for type-I censoring, which is the removal of unfailed units at pre-specified times. Confidence regions and intervals are calculated by use of the likelihood-ratio method.

This program was written by Timothy L. Krantz of the Vehicle Technology Center of the U.S. Army Research Laboratory for Glenn Research Center. Further information is contained in a TSP (see page 1).

Inquiries concerning rights for the commercial use of this invention should be addressed to NASA Glenn Research Center, Commercial Technology Office, Attn: Steve Fedor, Mail Stop 4-8, 21000 Brookpark Road, Cleveland, Ohio 44135. Refer to LEW-17401-1.

Comprehensive Micromechanics-Analysis Code — Version 4.0

Version 4.0 of the Micromechanics Analysis Code With Generalized Method of Cells (MAC/GMC) has been developed as an improved means of computational simulation of advanced composite materials. The previous version of MAC/GMC was described in “Comprehensive Micromechanics-Analysis Code” (LEW-16870), *NASA Tech Briefs*, Vol. 24, No. 6 (June 2000), page 38. To recapitulate: MAC/GMC is a computer program that predicts the elastic and inelastic thermomechanical responses of continuous and discontinuous composite materials with arbitrary internal microstructures and reinforcement shapes. The predictive capability of MAC/GMC rests on a model known as the generalized method of cells (GMC) — a continuum-based model of micromechanics that provides closed-form expressions for the macroscopic response of a composite material in terms of the properties, sizes, shapes, and responses of the individual constituents or phases that make up the material. Enhancements in version 4.0 include a capability for modeling thermomechanically and electromagnetically coupled

(“smart”) materials; a more-accurate (high-fidelity) version of the GMC; a capability to simulate discontinuous plies within a laminate; additional constitutive models of materials; expanded yield-surface-analysis capabilities; and expanded failure-analysis and life-prediction capabilities on both the microscopic and macroscopic scales.

This program was written by S. M. Arnold of Glenn Research Center and B. A. Bednarczyk of Ohio Aerospace Institute. Further information is contained in a TSP (see page 1).

Inquiries concerning rights for the commercial use of this invention should be addressed to NASA Glenn Research Center, Commercial Technology Office, Attn: Steve Fedor, Mail Stop 4-8, 21000 Brookpark Road, Cleveland, Ohio 44135. Refer to LEW-17495-1.

Component-Based Visualization System

A software system has been developed that gives engineers and operations personnel with no “formal” programming expertise, but who are familiar with the Microsoft Windows operating system, the ability to create visualization displays to monitor the health and performance of aircraft/spacecraft. This software system is currently supporting the X38 V201 spacecraft component/system testing and is intended to give users the ability to create, test, deploy, and certify their sub-system displays in a fraction of the time that it would take to do so using previous software and programming methods. Within the visualization system there are three major components: the developer, the deployer, and the widget set. The developer is a blank canvas with widget menu items that give users the ability to easily create displays. The deployer is an application that allows for the deployment of the displays created using the developer application. The deployer has additional functionality that the developer does not have, such as printing of displays, screen captures to files, windowing of displays, and also serves as the interface into the documentation archive and help system. The third major component is the widget set. The widgets are the visual representation of the items that will make up the display (i.e., meters, dials, buttons, numerical indicators, string indicators, and the like). This software was developed using Visual C++ and

uses COTS (commercial off-the-shelf) software where possible.

This program was written by Francisco Delgado of Johnson Space Center. For further information, contact the Johnson Technology Transfer Office at (281) 483-3809. MSC-23490

Software for Engineering Simulations of a Spacecraft

Spacecraft Engineering Simulation II (SES II) is a C-language computer program for simulating diverse aspects of operation of a spacecraft characterized by either three or six degrees of freedom. A functional model in SES can include a trajectory flight plan; a submodel of a flight computer running navigational and flight-control software; and submodels of the environment, the dynamics of the spacecraft, and sensor inputs and outputs. SES II features a modular, object-oriented programming style. SES II supports event-based simulations, which, in turn, create an easily adaptable simulation environment in which many different types of trajectories can be simulated by use of the same software. The simulation output consists largely of flight data. SES II can be used to perform optimization and Monte Carlo dispersion simulations. It can also be used to perform simulations for multiple spacecraft. In addition to its generic simulation capabilities, SES offers special capabilities for space-shuttle simulations: for this purpose, it incorporates submodels of the space-shuttle dynamics and a C-language version of the guidance, navigation, and control components of the space-shuttle flight software.

This program was written by Kirk Shireman and Gene McSwain of Johnson Space Center, and Bernell McCormick and Panayiotis Fardelos of the Boeing Co. For further information, contact the Johnson Technology Transfer Office at (281) 483-3809. MSC-23537

LabVIEW Interface for PCI-SpaceWire Interface Card

This software provides a LabView interface to the NT drivers for the PCI-SpaceWire card, which is a peripheral component interface (PCI) bus interface that conforms to the IEEE-1355/SpaceWire standard. As SpaceWire grows in popularity, the ability to use SpaceWire links within LabVIEW will be important to electronic ground support equipment vendors. In addition, there is a need for a high-level LabVIEW interface to the low-level device-driver software supplied with the card.

The LabVIEW virtual instrument (VI) provides graphical interfaces to support all (1) SpaceWire link functions, including message handling and routing; (2) monitoring as a passive “tap” using specialized hardware; and (3) low-level access to satellite mission-control subsystem functions. The software is supplied in a zip file that contains LabVIEW VI files, which provide various functions of the PCI-SpaceWire card, as well as higher-link-level functions. The VIs are suitably named according to the matching function names in the driver manual. A number of test programs also are provided to exercise various functions.

This work was done by James Lux, Frank Loya, and Alex Bachmann of Caltech for NASA’s Jet Propulsion Laboratory. Further information is contained in a TSP (see page 1).

This software is available for commercial licensing. Please contact Karina Edmonds of the California Institute of Technology at (818) 393-2827. Refer to NPO-35207.

Path Following With Slip Compensation for a Mars Rover

A software system for autonomous operation of a Mars rover is composed of several key algorithms that enable the rover to accurately follow a designated path, compensate for slippage of its wheels on terrain, and reach intended goals. The techniques implemented by the algorithms are visual odometry, full vehicle kinematics, a Kalman filter, and path following with slip compensation. The visual-odometry algorithm tracks distinctive scene features in stereo imagery to estimate rover motion between successively acquired stereo image pairs, by use of a maximum-likelihood motion-estimation algorithm. The full-vehicle kinematics algorithm estimates motion, with a no-slip assumption, from measured wheel rates, steering angles, and angles of rockers and bogies in the rover suspension system. The Kalman filter merges data from an inertial measurement unit (IMU) and the visual-odometry algorithm. The merged estimate is then compared to the kinematic estimate to determine whether and how much slippage has occurred. The kinematic estimate is used to complement the Kalman-filter estimate if no statistically significant slippage has occurred. If slippage has occurred, then a slip vector is calculated by subtracting the current Kalman filter estimate from the kinematic estimate. This slip vector is then used, in conjunction with the inverse

kinematics, to determine the wheel velocities and steering angles needed to compensate for slip and follow the desired path.

This work was done by Daniel Helmick, Yang Cheng, Daniel Clouse, Larry Matthies, and Stergios Roumeliotis of Caltech for NASA’s Jet Propulsion Laboratory. Further information is contained in a TSP (see page 1).

This software is available for commercial licensing. Please contact Karina Edmonds of the California Institute of Technology at (818) 393-2827. Refer to NPO-40703.

International Space Station Electric Power System Performance Code — SPACE

The System Power Analysis for Capability Evaluation (SPACE) software analyzes and predicts the minute-by-minute state of the International Space Station (ISS) electrical power system (EPS) for upcoming missions as well as EPS power generation capacity as a function of ISS configuration and orbital conditions. In order to complete the Certification of Flight Readiness (CoFR) process — in which the mission is certified for flight — each ISS System must thoroughly assess every proposed mission to verify that the system will support the planned mission operations; SPACE is the sole tool used to conduct these assessments for the power system capability. SPACE is an integrated power system model that incorporates a variety of modules tied together with integration routines and graphical output. The modules include orbit mechanics, solar array pointing/shadowing/thermal and electrical, battery performance, and power management and distribution performance. These modules are tightly integrated within a flexible architecture featuring data-file-driven configurations, source- or load-driven operation, and event scripting. SPACE also predicts the amount of power available for a given system configuration, spacecraft orientation, solar-array-pointing conditions, orbit, and the like. In the source-driven mode, the model must assure that energy balance is achieved, meaning that energy removed from the batteries must be restored (or balanced) each and every orbit. This entails an optimization scheme to ensure that energy balance is maintained without violating any other constraints. In the load-driven mode, SPACE determines whether a given distributed, time-varying electrical load profile can be supported by the power system and will determine whether the system stays in energy balance. Load-driven

mode also is used to assess each space shuttle mission to ISS, in support of the CoFR process.

This work was done by Jeffrey Hojnicky, David McKissock, James Fincannon, Robert Green, Thomas Kerlake, Ann Delleur, Jeffrey Follo, Jeffrey Trudell, David J. Hoffman, Anthony Jannette, and Carlos Rodriguez for Glenn Research Center. Further information is contained in a TSP (see page 1).

Inquiries concerning rights for the commercial use of this invention should be addressed to NASA Glenn Research Center, Commercial Technology Office, Attn: Steve Fedor, Mail Stop 4-8, 21000 Brookpark Road, Cleveland, Ohio 44135. Refer to LEW-17067.

2 Software for Automation of Real-Time Agents, Version 2

Version 2 of Closed Loop Execution and Recovery (CLEaR) has been developed. The previous version was reported in "Software for Automation of Real-Time Agents" (NPO-21040), *NASA Tech Briefs*, Vol. 26, No. 7 (July 2002), page 34. To recapitulate: CLEaR is an artificial intelligence computer program for use in planning and execution of actions of autonomous agents, including, for example, Deep Space Network (DSN) antenna ground stations, robotic exploratory ground vehicles (rovers), robotic aircraft (UAVs), and robotic spacecraft. CLEaR automates the generation and execution of command sequences, monitoring the sequence execution, and modifying the command sequence in response to execution deviations and failures as well as new goals for the agent to achieve. The development of CLEaR has focused on the unification of planning and execution to increase the ability of the autonomous agent to perform under tight resource and time constraints coupled with uncertainty in how much of resources and time will be required to perform a task. This unification is realized by extending the traditional three-tier robotic control architecture by increasing the interaction between the software components that perform deliberation and reactive functions. The increase in interaction reduces the need to replan, enables earlier detection of the need to replan, and enables replanning to occur before an agent enters a state of failure.

This program was written by Forest Fisher, Tara Estlin, Daniel Gaines, Steve Schaffer, Caroline Chouinard, Barbara Engelhardt, Colette Wilklow, Darren Mutz, Russell Knight, Gregg Rabideau, and Steve Chien of Caltech, and Reid Simmons and David Apfelbaum of CMU for NASA's Jet Propulsion

Laboratory. *Further information is contained in a TSP (see page 1).*

This software is available for commercial licensing. Please contact Karina Edmonds of the California Institute of Technology at (818) 393-2827. Refer to NPO-30745.

2 Software for Optimizing Plans Involving Interdependent Goals

A computer program enables construction and optimization of plans for activities that are directed toward achievement of goals that are interdependent. Goal interdependence is defined as the achievement of one or more goals affecting the desirability or priority of achieving one or more other goals. This program is overlaid on the Automated Scheduling and Planning Environment (ASPEN) software system, aspects of which have been described in a number of prior *NASA Tech Briefs* articles. Unlike other known or related planning programs, this program considers interdependences among goals that can change between problems and provides a language for easily specifying such dependences. Specifications of the interdependences can be formulated dynamically and provided to the associated planning software as part of the goal input. Then an optimization algorithm provided by this program enables the planning software to reason about the interdependences and incorporate them into an overall objective function that it uses to rate the quality of a plan under construction and to direct its optimization search. In tests on a series of problems of planning geological experiments by a team of instrumented robotic vehicles (rovers) on new terrain, this program was found to enhance plan quality.

This program was written by Tara Estlin, Daniel Gaines, and Gregg Rabideau of Caltech for NASA's Jet Propulsion Laboratory. Further information is contained in a TSP (see page 1).

This software is available for commercial licensing. Please contact Karina Edmonds of the California Institute of Technology at (818) 393-2827. Refer to NPO-30735.

2 Computing Gravitational Fields of Finite-Sized Bodies

A computer program utilizes the classical theory of gravitation, implemented by means of the finite-element method, to calculate the near gravitational fields of bodies of arbitrary size, shape, and

mass distribution. The program was developed for application to a spacecraft and to floating proof masses and associated equipment carried by the spacecraft for detecting gravitational waves. The program can calculate steady or time-dependent gravitational forces, moments, and gradients thereof. Bodies external to a proof mass can be moving around the proof mass and/or deformed under thermoelastic loads. An arbitrarily shaped proof mass is represented by a collection of parallelepiped elements. The gravitational force and moment acting on each parallelepiped element of a proof mass, including those attributable to the self-gravitational field of the proof mass, are computed exactly from the closed-form equation for the gravitational potential of a parallelepiped. The gravitational field of an arbitrary distribution of mass external to a proof mass can be calculated either by summing the fields of suitably many point masses or by higher-order Gauss-Legendre integration over all elements surrounding the proof mass that are part of a finite-element mesh. This computer program is compatible with more general finite-element codes, such as NASTRAN, because it is configured to read a generic input data file, containing the detailed description of the finite-element mesh.

This program was written by Marco Quadrelli of Caltech for NASA's Jet Propulsion Laboratory. Further information is contained in a TSP (see page 1).

This software is available for commercial licensing. Please contact Karina Edmonds of the California Institute of Technology at (818) 393-2827. Refer to NPO-40651.

2 Custom Sky-Image Mosaics From NASA's Information Power Grid

yourSkyG is the second generation of the software described in "yourSky: Custom Sky-Image Mosaics via the Internet" (NPO-30556), *NASA Tech Briefs*, Vol. 27, No. 6 (June 2003), page 45. Like its predecessor, yourSkyG supplies custom astronomical image mosaics of sky regions specified by requesters using client computers connected to the Internet. Whereas yourSky constructs mosaics on a local multiprocessor system, yourSkyG performs the computations on NASA's Information Power Grid (IPG), which is capable of performing much larger mosaicking tasks. (The IPG is high-performance computation and data grid that integrates geographically distributed

computers, databases, and instruments.) A user of yourSkyG can specify parameters describing a mosaic to be constructed. yourSkyG then constructs the mosaic on the IPG and makes it available for downloading by the user. The complexities of determining which input images are required to construct a mosaic, retrieving the required input images from remote sky-survey archives, uploading the images to the computers on the IPG, performing the computations remotely on the Grid, and downloading the resulting mosaic from the Grid are all transparent to the user.

This program was written by Joseph Jacob, James Collier, Loring Craymer, and David Curkendall of Caltech for NASA's Jet Propulsion Laboratory. Further information is contained in a TSP (see page 1).

This software is available for commercial licensing. Please contact Karina Edmonds of the California Institute of Technology at (818) 393-2827. Refer to NPO-40761.

ANTLR Tree Grammar Generator and Extensions

A computer program implements two extensions of ANTLR (Another Tool for Language Recognition), which is a set of software tools for translating source codes between different computing languages. ANTLR supports predicated-LL(k) lexer and parser grammars, a notation for annotating parser grammars to direct tree construction, and predicated tree grammars. ["LL(k)" signifies "left-right, leftmost derivation with k tokens of look-ahead," referring to certain characteristics of a grammar.] One of the extensions is a syntax for tree transformations. The other extension is the generation of tree grammars from annotated parser or input tree grammars. These extensions can simplify the process of generating source-to-source language translators and they make possible an approach, called "polyphase parsing," to translation between computing languages. The typical approach to translator development is to identify

high-level semantic constructs such as "expressions," "declarations," and "definitions" as fundamental building blocks in the grammar specification used for language recognition. The polyphase approach is to lump ambiguous syntactic constructs during parsing and then disambiguate the alternatives in subsequent tree transformation passes. Polyphase parsing is believed to be useful for generating efficient recognizers for C++ and other languages that, like C++, have significant ambiguities.

This program was written by Loring Craymer of Caltech for NASA's Jet Propulsion Laboratory. Further information is contained in a TSP (see page 1).

This software is available for commercial licensing. Please contact Karina Edmonds of the California Institute of Technology at (818) 393-2827. Refer to NPO-30565.

Generic Kalman Filter Software

The Generic Kalman Filter (GKF) software provides a standard basis for the development of application-specific Kalman-filter programs. Historically, Kalman filters have been implemented by customized programs that must be written, coded, and debugged anew for each unique application, then tested and tuned with simulated or actual measurement data. Total development times for typical Kalman-filter application programs have ranged from months to weeks. The GKF software can simplify the development process and reduce the development time by eliminating the need to re-create the fundamental implementation of the Kalman filter for each new application. The GKF software is written in the ANSI C programming language. It contains a generic Kalman-filter-development directory that, in turn, contains a code for a generic Kalman filter function; more specifically, it contains a generically designed and generically coded implementation of linear, linearized, and extended Kalman filtering algorithms, including algo-

rithms for state- and covariance-update and -propagation functions. The mathematical theory that underlies the algorithms is well known and has been reported extensively in the open technical literature. Also contained in the directory are a header file that defines generic Kalman-filter data structures and prototype functions and template versions of application-specific subfunction and calling "navigation/estimation" routine code and headers. Once the user has provided a calling routine and the required application-specific subfunctions, the application-specific Kalman-filter software can be compiled and executed immediately. During execution, the generic Kalman-filter function is called from a higher-level "navigation" or "estimation" routine that preprocesses measurement data and postprocesses output data. The generic Kalman-filter function uses the aforementioned data structures and five implementation-specific subfunctions, which have been developed by the user on the basis of the aforementioned templates. The GKF software can be used to develop many different types of unfactored Kalman filters. A developer can choose to implement either a linearized or an extended Kalman filter algorithm, without having to modify the GKF software. Control dynamics can be taken into account or neglected in the filter-dynamics model. Filter programs developed by use of the GKF software can be made to propagate equations of motion for linear or nonlinear dynamical systems that are deterministic or stochastic. In addition, filter programs can be made to operate in user-selectable "covariance analysis" and "propagation-only" modes that are useful in design and development stages.

This program was written by Michael E. Lisano II and Edwin Z. Crues of LinCom for Johnson Space Center. For further information, contact the Johnson Technology Transfer Office at (281) 483-3809. MSC-23006



Alignment Stage for a Cryogenic Dilatometer

A low-friction, low-thermal-expansion kinematic design affords stability and precise adjustability.

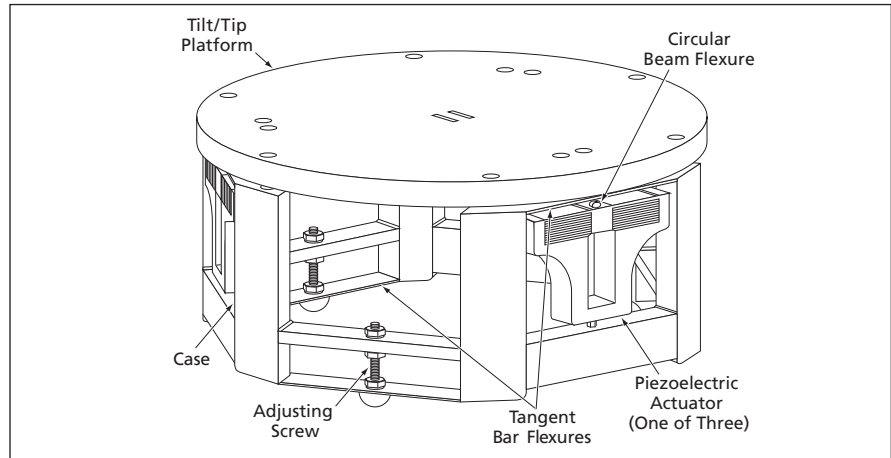
NASA's Jet Propulsion Laboratory, Pasadena, California

A three-degree-of-freedom alignment stage has been designed and built for use in a cryogenic dilatometer that is used to measure thermal strains. The alignment stage enables precise adjustments of the positions and orientations of optical components to be used in the measurements and, once adjustments have been completed, keeps the components precisely aligned during cryogenic-dilatometer operations that can last as long as several days.

The alignment stage (see figure) includes a case, a circular tilt/tip platform, and a variety of flexural couplings between the case and the platform, all machined from a single block of the low-thermal-expansion iron/nickel alloy Invar, in order to minimize effects of temperature gradients and to obtain couplings that are free of stiction and friction. There are three sets of flexural couplings clocked at equal angles of 120° around the platform, constituting a three-point kinematic support system.

Associated with the three sets of flexural couplings are three sets of two actuators each, also clocked at equal angles, which serve to deflect the couplings to adjust the platform in tilt, tip, and/or piston.

By use of actuator/flexural coupling sets that include tangent bar flexures and Invar screws and nuts, one can make coarse adjustments of axial displacement over a range of 1.79 mm with a resolution of 1 μm (corresponding to a tilt/tip angle range of 23.5 milliradians with resolution of about 13 microradians or perhaps somewhat less).



The **Alignment Stage** comprises a monolithic Invar structure that contains flexures plus screw and piezoelectric actuators that deform the flexures to effect adjustments.

Fine adjustments are made by use of piezoelectric actuators in combination with three different types of flexures that apply the proper axial preload and transmit the piezoelectric displacements to the platform while preventing the coupling of shear and bending loads, which could damage the piezoelectric actuators. The fine adjustments are characterized by axial displacement over a range of 15 μm with a resolution of 10 μm (corresponding to a tilt/tip angle range of 222.85 microradians with a resolution of about 0.15 nanoradian or perhaps somewhat less). The piezoelectric actuators are driven by circuits that are parts of a computer-based feedback tilt/tip/piston control system.

By virtue of the low thermal expansion of the monolithic Invar body and the

negative thermal expansion of the piezoelectric actuators, the alignment stage is athermalized to within about 7 picometers of axial displacement and 0.1 nanoradian of tip and/or tilt in the presence of an axial temperature gradient of 0.1 K across its structure. Inasmuch as all adjustments are symmetric about the center and are kinematic, any tip or tilt adjustment of the stage is made about its center, with minimal cross-coupling.

This work was done by Matthew Dudik and Donald Moore of Caltech for NASA's Jet Propulsion Laboratory. Further information is contained in a TSP (see page 1).

The software used in this innovation is available for commercial licensing. Please contact Karina Edmonds of the California Institute of Technology at (818) 393-2827. Refer to NPO-40390

Rugged Iris Mechanism

Advantages include capability for full obscuration, low friction, and general adaptability of design.

Goddard Space Flight Center, Greenbelt, Maryland

A rugged iris mechanism has been designed to satisfy several special requirements, including a wide aperture in the "open" position, full obscuration in the "closed" position, ability to function in a cryogenic or other harsh envi-

ronment, and minimization of friction through minimization of the number of components. An important element of the low-friction aspect of the design is maximization of the flatness of, and provision of small gaps between, adja-

cent iris blades. The tolerances of the design can be very loose, accommodating thermal expansions and contractions associated with large temperature excursions. The design is generic in that it is adaptable to a wide range of

aperture sizes and can be implemented in a variety of materials to suit the thermal, optical, and mechanical requirements of various applications.

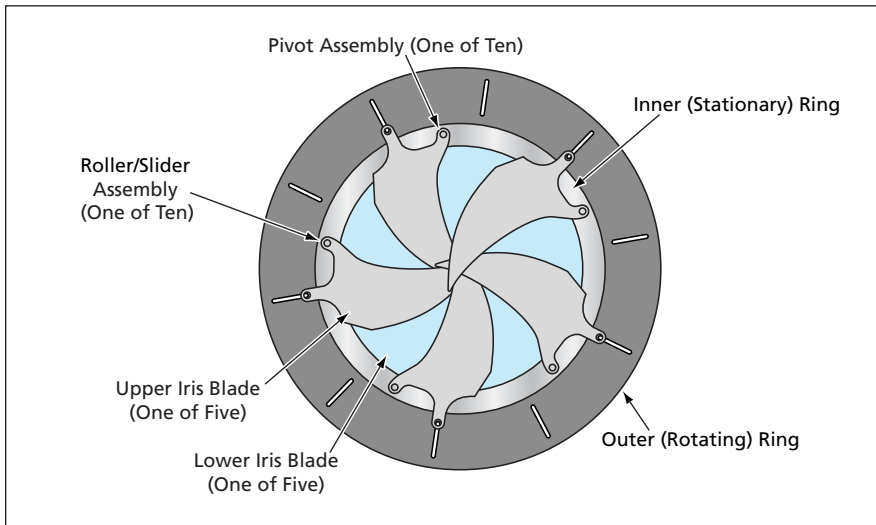
The mechanism (see figure) includes an inner flat ring, an outer flat ring, and

an even number of iris blades. The iris blades shown in front in the figure are denoted as "upper," and the iris blades shown partly hidden behind the front ones are denoted as "lower." Each iris blade is attached to the inner ring by a

pivot assembly and to the outer ring by a roller/slider assembly. The upper and lower rings are co-centered and are kept in sliding contact. The iris is opened or closed by turning the outer ring around the center while holding the inner ring stationary.

The mechanism is enclosed in a housing (not shown in the figure) that comprises an upper and a lower housing shell. The housing provides part of the sliding support for the outer ring and keeps the two rings aligned as described above. The aforementioned pivot assemblies at the inner ring also serve as spacers for the housing. The lower housing shell contains part of the lower sliding surface and features for mounting the overall mechanism and housing assembly. The upper housing shell contains part of the upper sliding surface.

This work was done by Nelson J. Ferragut of Goddard Space Flight Center. Further information is contained in a TSP (see page 1). GSC-14550



The Iris Is Opened or Closed by turning the outer ring with respect to the inner ring.

Treatments To Produce Stabilized Aluminum Mirrors for Cryogenic Uses

Selected heat treatments are performed between and after fabrication steps.

Goddard Space Flight Center, Greenbelt, Maryland

Five metallurgical treatments have been tested as means of stabilizing mirrors that are made of aluminum alloy 6061 and are intended for use in cryogenic applications. Aluminum alloy 6061 is favored as a mirror material by many scientists and engineers. Like other alloys, it shrinks upon cool-down from room temperature to cryogenic temperature. This shrinkage degrades the optical quality of the mirror surfaces. Hence, the metallurgical treatments were tested to determine which one could be most effective in minimizing the adverse optical effects of cool-down to cryogenic temperatures. Each of the five metallurgical treatments comprises a multistep process, the steps of which are interspersed with the steps of the mirror-fabrication process. The five metallurgical-treatment/fabrication-process combinations were compared with each other and with a benchmark fabrication process, in which a mirror is made from an alloy blank by (1) symmetrical rough machining, (2) finish machining to within 0.006 in. (≈ 0.15 mm) of

final dimensions, and finally (3) diamond turning to a mirror finish. Two specimens — a flat mirror and a spherical mirror — were fabricated in each case. The blanks for all the specimens were cut from the same plate of aluminum alloy 6061-T651. (The suffix “T651” denotes a stress-relieving treatment that involves reducing residual stresses by mechanical stretching of the previously untreated alloy.) Of the five metallurgical-treatment/fabrication-process combinations tested, the one found to exert the greatest stabilizing effect comprises the following ten steps:

1. Rough machining.
2. Solution heat treatment at a temperature of 985 °F (≈ 529 °C).
3. Quench within 15 s in a solution of 28 percent UCON Quenchant A (or an equivalent aqueous quenching liquid) at a temperature of 90 °F (≈ 32 °C).
4. Uphill quench: Allow to reach room temperature, slowly dip into a tank of liquid nitrogen followed by rapid immersion in a tank of boiling water.
5. Age at 350 °F (≈ 177 °C).

6. Finish machine leaving about 0.006 in. (0.15 mm) for polishing.
7. Age again as in step 5.
8. Three thermal cycles with heating and cooling rates not to exceed 3 °F/min (1.7 °C/min) as follows: Cool to -310 °F (-190 °C), hold for 30 min, heat to room temperature, hold for 15 min, heat to 300 °F (150 °C), hold for 15 minutes, and cool to room temperature.
9. Diamond turning/polishing.
10. Three thermal cycles as in step 7.

Separate tests showed that forged AL6061 with the same processing method would yield slightly better mirrors than those made from AL6061-T651 plates.

This work was done by Wahid Zewari, Michael Barthelmy, and Raymond Ohl of Goddard Space Flight Center. Further information is contained in a TSP (see page 1).

Inquiries concerning rights for the commercial use of this invention should be addressed to the Patent Counsel, Goddard Space Flight Center, (301) 286-7351. Refer to GSC-14736-1.

Making AlN_x Tunnel Barriers Using a Low-Energy Nitrogen-Ion Beam

Ion-beam parameters can be controlled to optimize properties of AlN_x layers.

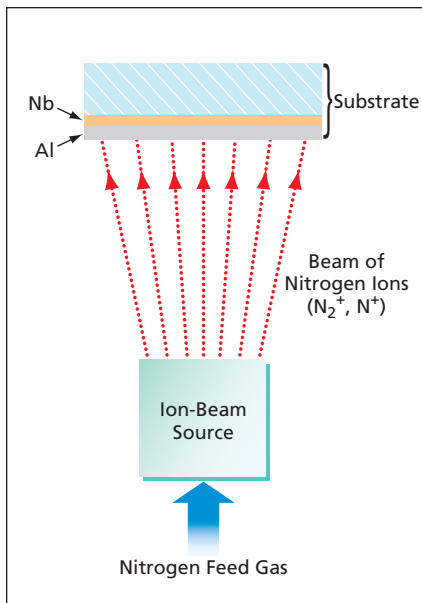
NASA's Jet Propulsion Laboratory, Pasadena, California

A technique based on accelerating positive nitrogen ions onto an aluminum layer has been demonstrated to be effective in forming thin (<2 nm thick) layers of aluminum nitride (AlN_x) for use as tunnel barriers in Nb/Al- AlN_x /Nb superconductor/insulator/superconductor (SIS) Josephson junctions. AlN_x is the present material of choice for tunnel barriers because, to a degree greater than that of any other suitable material, it offers the required combination of low leakage current at high current density and greater thermal stability.

While ultra-thin AlN films with good thickness and stoichiometry control are easily formed using techniques such as reactive molecular beam epitaxy and chemical vapor deposition, growth temperatures of 900 °C are necessary for the dissociative adsorption of nitrogen from either nitrogen (N_2) or ammonia (NH_3). These growth temperatures are prohibitively high for the formation of tunnel barriers on Nb films because interfacial reactions at temperatures as low as 200 to 300 °C degrade device properties. Heretofore, deposition by reactive sputtering and nitridation of thin Al lay-

ers with DC and RF nitrogen plasmas have been successfully used to form AlN barriers in SIS junctions. However, precise control over critical current density J_c has proven to be a challenge, as is attaining adequate process reproducibility from system to system.

The present ion-beam technique is an alternative to the plasma or reactive sputtering techniques as it provides a highly controlled arrival of reactive species, independent of the electrical conditions of the substrate or vacuum chamber. Independent and accurate control of parameters such as ion en-



The Beam of Nitrogen Ions impinges on the aluminum substrate surface layer, forming an ultra-thin layer of AlN_x.

ergy, flux, species, and direction promises more precise control of film characteristics such as stoichiometry and thickness than is the case with typical plasma processes. In particular, the background pressure during ion-beam nitride growth is 2 or 3 orders of magnitude lower, minimizing the formation of compounds with contaminants,

which is critical in devices the performance of which is dictated by interfacial characteristics. In addition, the flux of incoming species can be measured *in situ* using ion probes so that the dose can be controlled accurately.

The apparatus used in the present ion-beam technique includes a vacuum chamber containing a commercial collimated-ion-beam source, a supply of nitrogen and argon, and an ion probe for measuring the ion dose. Either argon or nitrogen can be used as the feed gases for the ion source, depending on whether cleaning of the substrate or growth of the nitride, respectively, is desired. Once the Nb base electrode and Al proximity layer have been deposited, the N₂ gas line to the ion beam is vented and purged, and the ion-source is turned on until a stable discharge is obtained. The substrate is moved over the ion-beam source to expose the Al surface layer to the ion beam (see figure) for a specified duration for the formation of the nitride tunnel barrier. Next, the Nb counter-electrode layer is deposited on the nitride surface layer. The Nb/Al-AlN_x/Nb-trilayer-covered substrate is then patterned into individual devices by use of conventional integrated-circuit processing techniques.

A wide parameter space was investi-

gated over which devices were fabricated reproducibly and with high quality. The hysteretic nature of the current-voltage characteristic along with the high subgap ratio indicate the incident nitrogen ions chemically reacted with the Al layer as expected, to form a continuous AlN_x barrier. Chemical analysis of the barrier performed using x-ray photoelectron-spectroscopy confirmed the presence of AlN_x. Critical current density J_c ranged from 550 to 9,400 A/cm² with subgap-to-normal resistance ratios ranging from 50 to 12.6. The J_c was found to decrease with increasing dose and increasing beam energy. The run-to-run reproducibility was determined to be very good. The spatial variation of the ion current density was also measured and correlated with J_c over a 76-mm Si wafer. The junctions were also found to be stable on annealing up to temperatures of 250 °C. This technique could be applied to form other metal nitrides at room temperatures for device applications where a high degree of control is desired.

This work was done by Anupama Kaul, Alan Kleinsasser, Bruce Bumble, Henry LeDuc, and Karen Lee of Caltech for NASA's Jet Propulsion Laboratory. Further information is contained in a TSP (see page 1). NPO-41297

Making Wide-IF SIS Mixers With Suspended Metal-Beam Leads

Devices are fabricated on SOI substrates by use of silicon-micromachining techniques.

NASA's Jet Propulsion Laboratory, Pasadena, California

A process that employs silicon-on-insulator (SOI) substrates and silicon (Si) micromachining has been devised for fabricating wide-intermediate-frequency-band (wide-IF) superconductor/insulator/superconductor (SIS) mixer devices that result in suspended gold beam leads used for radio-frequency grounding. The mixers are formed on 25- μ m-thick silicon membranes. They are designed to operate in the 200 to 300 GHz frequency band, wherein wide-IF receivers for tropospheric-chemistry and astrophysical investigations are necessary.

The fabrication process can be divided into three sections:

1. The front-side process, in which SIS devices with beam leads are formed on a SOI wafer;
2. The backside process, in which the

SOI wafer is wax-mounted onto a carrier wafer, then thinned, then partitioned into individual devices; and

3. The release process, in which the individual devices are separated using a lithographic dicing technique.

The total thickness of the starting 4-in. (10.16-cm)-diameter SOI wafer includes 25 μ m for the Si device layer, 0.5 μ m for the buried oxide (BOX) layer, and 350 μ m for the Si-handle layer. The front-side process begins with deposition of an etch-stop layer of SiO₂ or AlN_x, followed by deposition of a Nb/Al-AlN_x/Nb trilayer in a load-locked DC magnetron sputtering system. The lithography for four of a total of five layers is performed in a commercial wafer-stepping apparatus. Diagnostic test dies are patterned concurrently at certain locations on the wafer, alongside the mixer

devices, using a different mask set. The conventional, self-aligned lift-off process is used to pattern the SIS devices up to the wire level.

The beam-leads are formed as extensions from the SIS devices by using a bilayer lift-off process with poly(methyl methacrylate) [PMMA] and photoresist. After defining the beam-leads, the interfacial layer between the PMMA and photoresist is etched in an oxygen plasma. Ultraviolet irradiation is used to expose the PMMA, which is then developed in chlorobenzene. The wafer is then placed in the sputtering system, where a seed layer of Nb/Au is deposited to enhance adhesion. The Au beam leads are grown to the desired thickness in an electron-beam evaporation system. After deposition, the unwanted gold is easily removed by lift-off in acetone.

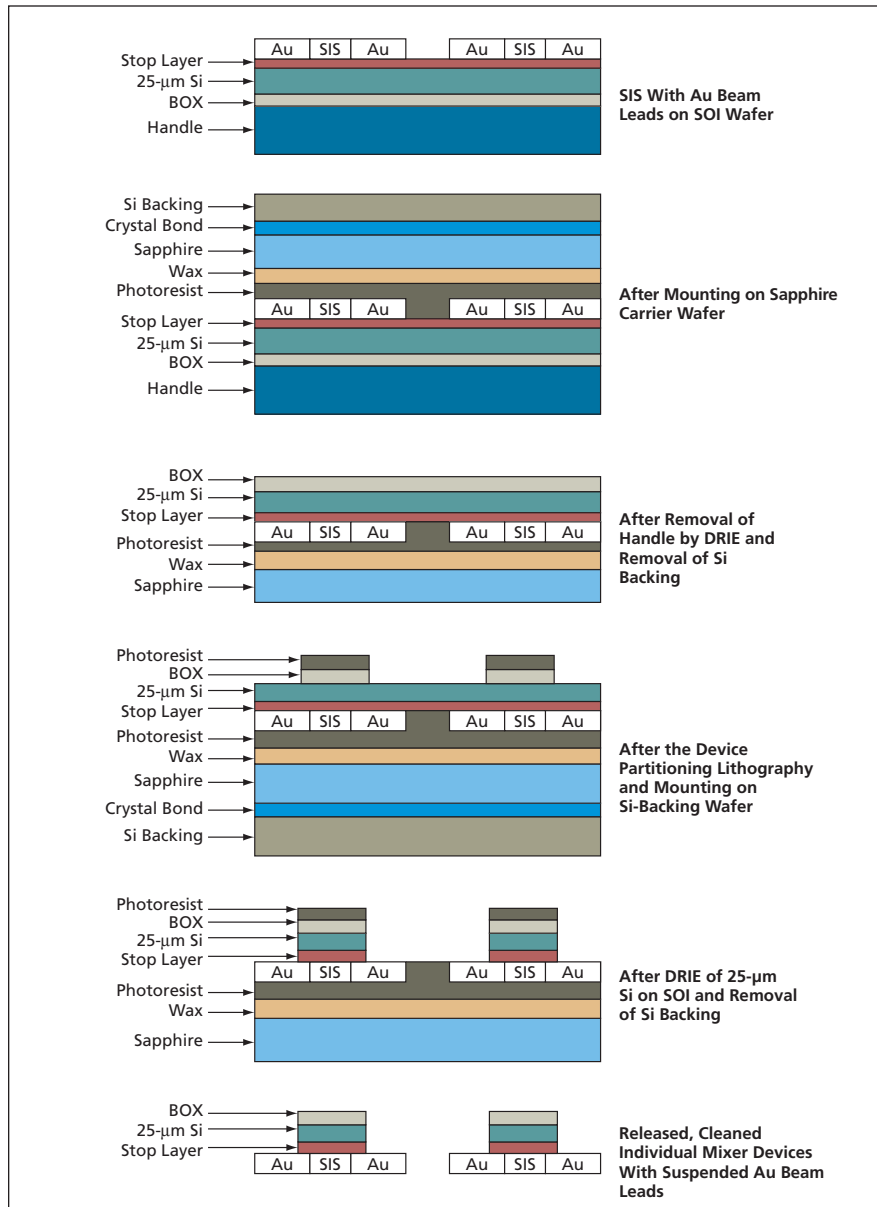
In the next step, the backside process is initiated by wax mounting the SOI wafer onto a sapphire carrier wafer, as illustrated in the figure. The 350 μm Si-

handle layer of the SOI wafer is removed by deep-trench reactive-ion etching (DRIE). Now further lithography is necessary on the 25 μm thick Si membrane

layer that is held down onto a 4-in. (10.16-cm) wafer by a relatively high-melting-point wax. If the cooling on the DRIE system is not sufficient during the etching of the handle layer, the wax would start to flow at $\sim 85^\circ\text{C}$, causing the Si membrane to wrinkle, which would prevent any backside lithography to be performed. A contact aligner is used to pattern the now-exposed 25- μm thick Si layer in order to partition the devices into individual mixers. Since an anisotropic etch is desired for patterning the 25- μm thick Si membrane, the DRIE apparatus is operated in the pulsed mode where SF_6 and C_2F_4 are flowed intermittently. The devices are then released by dissolving the front-side protection resist in acetone, followed by soaking in an N-methyl-pyrrolidone-based solution, which removes any residual photoresist. The devices are finally dipped in IPA.

Electrical measurements of the devices was performed at 4.2 K. Measurements were performed on devices that were on thinned 25- μm Si membranes and those devices where the handle layer was not removed. No change in device parameters such as current density (J_c), gap voltage, and sub-gap leakage current was observed, indicating the backside process did not introduce any thermal excursions, which would have been evident from increased leakage currents and reduced gap voltages. In addition, the J_c on the individual mixer chips correlated to the J_c that was measured on devices from the diagnostic chip. The data suggest that this wax-mounted backside lithography beam-lead process is compatible with conventional SIS device fabrication technology.

This work was done by Anupama Kaul, Bruce Bumble, Karen Lee, Henry LeDuc, Frank Rice, and Jonas Zmuidzinas of Caltech for NASA's Jet Propulsion Laboratory. Further information is contained in a TSP (see page 1). NPO-41296



In the **Backside and Release Processes**, the SOI wafer is thinned and partitioned into individual devices, which are then released. Some of the layers depicted and subprocesses mentioned here are omitted from the main text for the sake of brevity.



Sol-Gel Glass Holographic Light-Shaping Diffusers

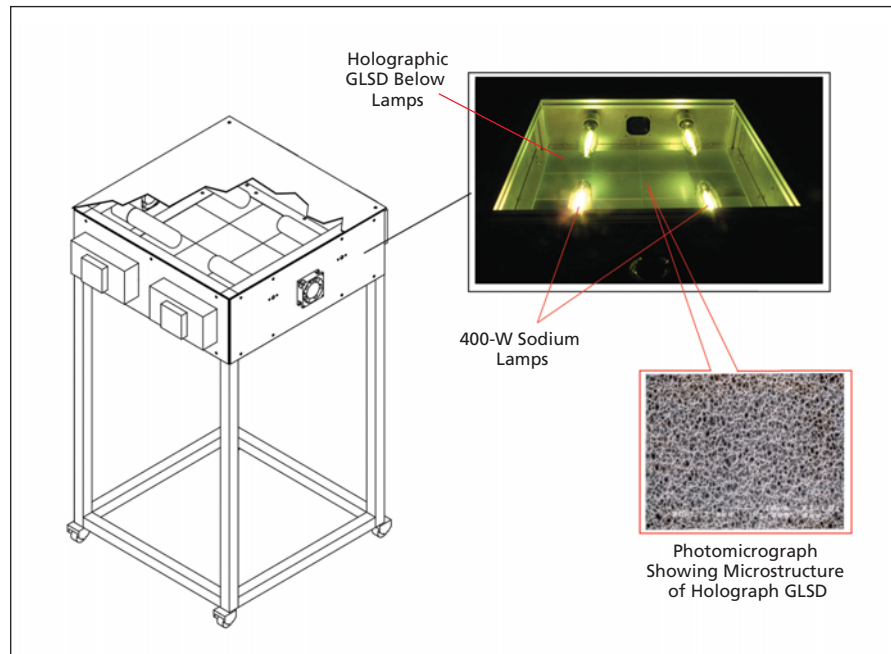
Defined areas can be illuminated diffusely with high efficiency.

John F. Kennedy Space Center, Florida

Holographic glass light-shaping diffusers (GLSDs) are optical components for use in special-purpose illumination systems (see figure). When properly positioned with respect to lamps and areas to be illuminated, holographic GLSDs efficiently channel light from the lamps onto specified areas with specified distributions of illumination — for example, uniform or nearly uniform irradiance can be concentrated with intensity confined to a peak a few degrees wide about normal incidence, over a circular or elliptical area.

Holographic light diffusers were developed during the 1990s. The development of the present holographic GLSDs extends the prior development to incorporate sol-gel optical glass. To fabricate a holographic GLSD, one records a hologram on a sol-gel silica film formulated specially for this purpose. The hologram is a quasi-random, micro-sculpted pattern of smoothly varying changes in the index of refraction of the glass. The structures in this pattern act as an array of numerous miniature lenses that refract light passing through the GLSD, such that the transmitted light beam exhibits a precisely tailored energy distribution.

In comparison with other light diffusers, holographic GLSDs function with remarkably high efficiency: they typically transmit 90 percent or more of the incident lamp light onto the designated areas. In addition, they can withstand temperatures in excess of 1,000 °C. These characteristics make holographic GLSDs attractive for use in diverse lighting applications that involve high temperatures and/or re-



The **Holographic GLSD** in this lighting system concentrates and diffuses light from four lamps onto the framed area below. This lighting system is designed specifically for illumination experiments on growing plants under controlled conditions.

quirements for high transmission efficiency for ultraviolet, visible, and near-infrared light. Examples include projectors, automobile headlights, aircraft landing lights, high-power laser illuminators, and industrial and scientific illuminators.

This work was done by Kevin Yu, Kang Lee, Gajendra Savant, and Khin Swe (Lillian) Yin of Physical Optics Corp. for Kennedy Space Center.

In accordance with Public Law 96-517, the contractor has elected to retain title to this

invention. Inquiries concerning rights for its commercial use should be addressed to:

*Kevin Yu
Physical Optics Corp., Electro-Optics
Holography Division
20600 Gramercy Place, Building 100
Torrance, CA 90501-1821
Phone No. (310) 320-3088 X117*

Refer to KSC-12436, volume and number of this NASA Tech Briefs issue, and the page number.

Automated Counting of Particles To Quantify Cleanliness

Lyndon B. Johnson Space Center, Houston, Texas

A machine vision system, similar to systems used in microbiological laboratories to count cultured microbes, has been proposed for quantifying the cleanliness of nominally precisely cleaned hardware by counting residual contaminant particles. The system would include a microscope equipped

with an electronic camera and circuitry to digitize the camera output, a personal computer programmed with machine-vision and interface software, and digital storage media. A filter pad, through which had been aspirated solvent from rinsing the hardware in question, would be placed on the mi-

croscope stage. A high-resolution image of the filter pad would be recorded. The computer would analyze the image and present a histogram of sizes of particles on the filter. On the basis of the histogram and a measure of the desired level of cleanliness, the hardware would be accepted or re-

jected. If the hardware were accepted, the image would be saved, along with other information, as a quality record. If the hardware were rejected, the histogram and ancillary information would be recorded for analysis of

trends. The software would perceive particles that are too large or too numerous to meet a specified particle-distribution profile. Anomalous particles or fibrous material would be flagged for inspection.

This work was done by James Rhodes of Lockheed Martin Corp. for Johnson Space Center. For further information, contact the Johnson Technology Transfer Office at (281) 483-3809. MSC-23836

Phase Correction for GPS Antenna With Nonunique Phase Center

Position can be determined more accurately.

Lyndon B. Johnson Space Center, Houston, Texas

A method of determining the position and attitude of a body equipped with a Global Positioning System (GPS) receiver includes an accounting for the location of the nonunique phase center of a distributed or wraparound GPS antenna. The method applies, more specifically, to the case in which (1) the GPS receiver utilizes measurements of the phases of GPS carrier signals in its position and attitude computations and (2) the body is axisymmetric (e.g., spherical or round cylindrical) and wrapped at its equator with a single- or multiple-element antenna, the radiation pattern of which is also axisymmetric with the same axis of symmetry as that of the body.

The figure depicts the geometric relationships among the GPS-equipped object centered at position \mathbf{r}_B , the i th GPS satellite at position \mathbf{r}_{si} , and the phase center at position \mathbf{r}_{pi} relative to the center of the body during observation of the i th satellite. The main GPS observable calculated from the phase measurement for the i th satellite is the pseudorange $\|\mathbf{v}_i\|$,

which is nominally the distance from the phase center to the i th satellite. However, what is needed to determine the position of the center of the body is another pseudorange — that which one would obtain if the phase center were at the center of the body. That pseudorange would nominally equal $\|\mathbf{r}_{si} - \mathbf{r}_B\|$. In order to determine $\|\mathbf{r}_{si} - \mathbf{r}_B\|$ from phase measurements, it is necessary to account for the phase difference attributable to \mathbf{r}_{pi} .

A straightforward mathematical derivation that starts with the law of cosines for this geometry and that incorporates simplifying assumptions based on the axisymmetry and on the smallness of $\|\mathbf{r}_{pi}\|$ relative to $\|\mathbf{r}_{si} - \mathbf{r}_B\|$ leads to the following equations:

$$\|\mathbf{r}_{si} - \mathbf{r}_B\| = \|\mathbf{v}_i\| + \|\mathbf{r}_{pi}\| \cos(\beta_i) \quad (1)$$

$$\text{and} \quad \cos(\beta_i) = \left[1 - (\hat{\mathbf{r}}_{sib} \cdot \hat{\mathbf{z}}_B)^2 \right]^{1/2} \quad (2)$$

where

- β_i is the angle between $\mathbf{r}_{si} - \mathbf{r}_B$ and \mathbf{r}_{pi} as shown in the figure,
- $\hat{\mathbf{z}}_B$ is the unit vector along the axis of

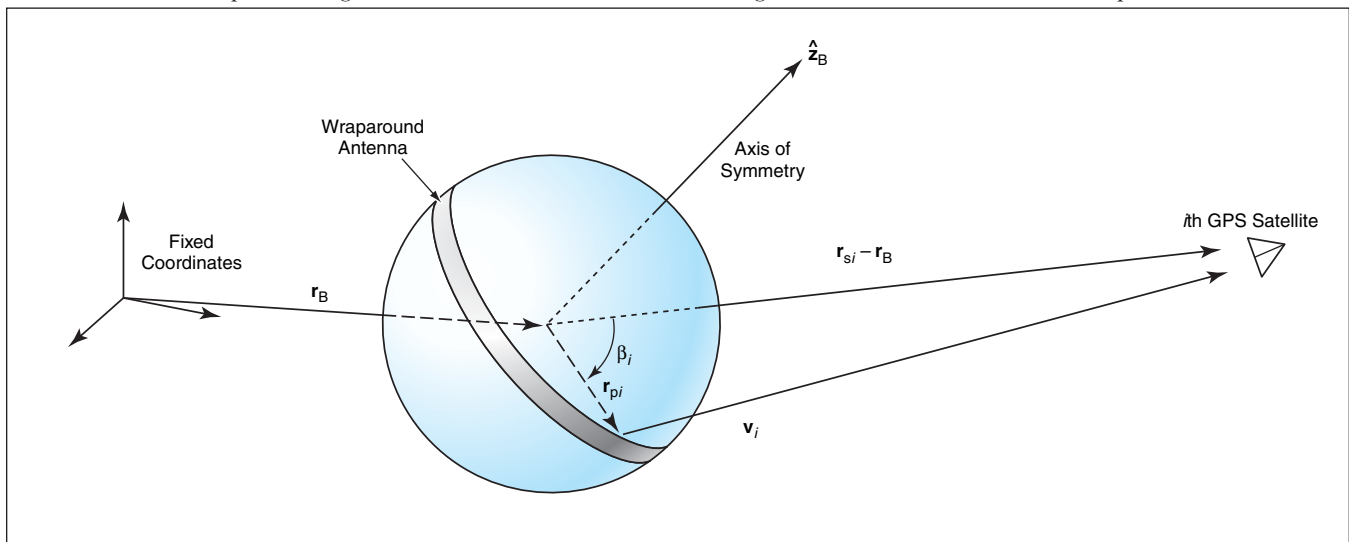
symmetry as shown in the figure, and

$$\hat{\mathbf{r}}_{sib} \equiv \left(\frac{\mathbf{r}_{si} - \mathbf{r}_B}{\|\mathbf{r}_{si} - \mathbf{r}_B\|} \right)$$

is the unit vector along $\mathbf{r}_{si} - \mathbf{r}_B$.

The computation of the desired pseudorange $\|\mathbf{r}_{si} - \mathbf{r}_B\|$ begins with a coarse estimate of \mathbf{r}_B — for example, a previously computed value or a value computed anew without the phase correction. The coarse estimate of \mathbf{r}_B is used to obtain an estimate of $\hat{\mathbf{r}}_{sib}$, which is used in iterations of equation 1 to obtain successively refined estimates of \mathbf{r}_B . Optionally, one can also obtain successively refined estimates of $\hat{\mathbf{r}}_{sib}$ from the iterations, though in most GPS applications, the error in the initial estimate of $\hat{\mathbf{r}}_{sib}$ should be negligible.

The iterations follow one of two courses, depending on whether or not $\|\mathbf{r}_{pi}\|$ and the attitude of the body are known *a priori*. If the attitude is known, then $\hat{\mathbf{z}}_B$ is known and can be inserted in equation 2, which yields $\cos(\beta_i)$ for use in equation 1. Then $\|\mathbf{r}_{pi}\|$ and $\cos(\beta_i)$ can be used in equation 1 without fur-



An Axisymmetric Body With a Wraparound GPS Antenna at its equator contains a GPS receiver that measures the phase of the signal from the i th GPS satellite at a nonunique phase center at position vector \mathbf{r}_{pi} relative to the center of the body. For simplicity, $\|\mathbf{r}_{pi}\|$ is depicted as equal to the radius of the wraparound antenna, but it could differ.

ther ado. If $\|\mathbf{r}_{pi}\|$ and $\hat{\mathbf{z}}_B$ are not known *a priori*, then it is necessary to determine $\|\mathbf{r}_{pi}\|$, the attitude, and the phase-correction term $\|\mathbf{r}_{pi}\|\cos(\beta_i)$ from a least-squares or other fit of (a) an approximate geometric model of the

amount by which the phase at \mathbf{r}_{pi} leads the phase at \mathbf{r}_B to (b) phase measurements for all of the GPS signals detected by the receiver.

This work was done by Patrick W. Fink and Justin Dobbins of Johnson Space Center.

This invention is owned by NASA, and a patent application has been filed. Inquiries concerning nonexclusive or exclusive license for its commercial development should be addressed to the Patent Counsel, Johnson Space Center, (281) 483-0837. Refer to MSC-23228.

Compact Infrasonic Windscreen

High values of infrasound-transmission and wind-noise-attenuation coefficients can be realized.

Langley Research Center, Hampton, Virginia

A compact windscreen has been conceived for a microphone of a type used outdoors to detect atmospheric infrasound from a variety of natural and man-made sources. Wind at the microphone site contaminates received infrasonic signals (defined here as sounds having frequencies <20 Hz), because a microphone cannot distinguish between

infrasonic pressures (which propagate at the speed of sound) and convective pressure fluctuations generated by wind turbulence. Hence, success in measurement of outdoor infrasound depends on effective screening of the microphone from the wind.

To be effective, an infrasonic windscreen must fulfill four basic require-

ments: (1) it must attenuate noise generated by ambient wind, (2) it must transmit infrasound propagating across the microphone, (3) it must be useable in all weather, and (4) it must not be susceptible to generation of infrasound through shedding of vortices.

Past methods of wind screening include the use of cloth or open-cell foam, and the use of an array of pipes. A windscreen made of cloth or open-cell foam is thought to break up incident airflow into very small turbulent eddies that dissipate wind energy in the form of heat. Such a windscreen is effective at audio frequencies (>20 Hz) but not at infrasonic frequencies (<20 Hz).

An array of pipes used as a windscreen consists, more specifically, of several perforated pipes, called a "spider," fanning out radially from a microphone situated in an enclosed housing. The array is vast — covering an area comparable to that of an athletic field — and its performance as a windscreen is degraded by resonances that depend on the lengths of the pipes.

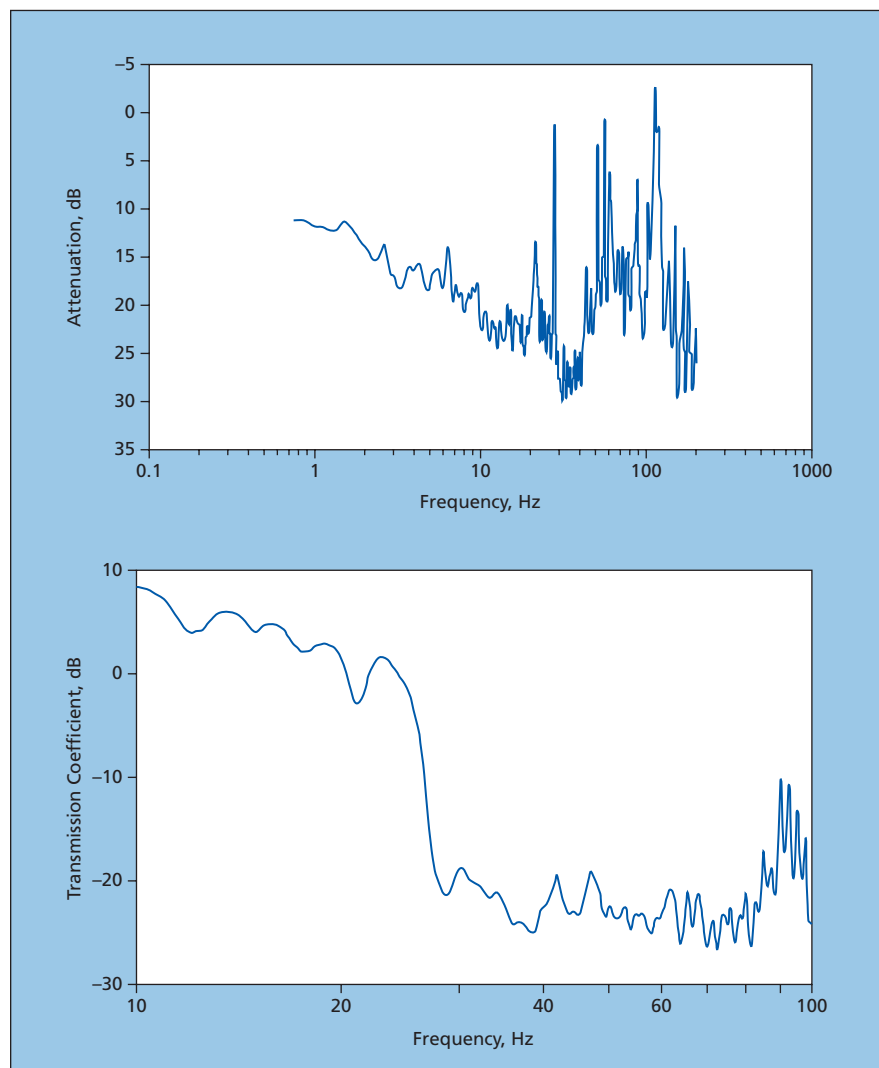


Figure 1. These Plots Are Results of Tests of the wind-noise-attenuation and infrasound-transmission properties of a polyurethane-foam windscreen.



Figure 2. A Cylindrical Windscreen Covers a Microphone mounted on a pole outdoors.

The present compact windscreen is based on an entirely different principle: that infrasound at sufficiently large wavelength can penetrate any barrier of practical thickness. Thus, a windscreen having solid, non-porous walls can block connected pressure fluctuations from the wind while transmitting infrasonic acoustic waves. The transmission coefficient depends strongly upon the ratio between the acoustic impedance of the windscreen and that of air. Several materials have been found to have impedance ratios that render them suitable for use in constructing walls that have practical thicknesses and are capable of high transmission of infrasound. These materials (with their impedance ratios in parentheses) are polyurethane foam (222), space-shuttle tile material (332), balsa (323), cedar (3,151), and pine (4,713).

A small wind tunnel was built to test the acoustical properties of a variety of windscreen materials. A fan generated wind at speeds up to 21 mph (9.4 m/s) across an infrasonic microphone. Tests were conducted with and without the windscreen; the difference in the noises detected in

the presence and absence of the windscreen was used as a measure of the attenuation of wind noise by the windscreen.

The windscreen that performed best in the wind-tunnel tests was a cylinder made of polyurethane foam of a type known in the industry as “eight-pounder,” having an inside diameter of 3 in. (7.62 cm), a wall thickness of 0.5 in. (1.27 cm), and a length of 12 in. (30.48 cm). The attenuation of wind-generated noise was quantified as the ratio between the wind noises measured without and with this windscreen. The results, plotted in the upper part of Figure 1, show that this windscreen attenuated wind noise by amounts ranging from 12 to 20 dB at frequencies ranging from 0.7 to 20 Hz. The large spikes in the spectrum represent aeolian tones generated by the wind passing over the windscreen, but these lie above the infrasonic range.

For measurements of the infrasonic-transmission coefficient of this windscreen, a subwoofer was placed at an end of the wind tunnel and used to generate a tone that was swept over the frequency band from 10 to 200 Hz. In this case, the

ratio between detected sounds, with and without the windscreen, was taken as a measure of the transmission through the windscreen. The results for the portion of the spectrum from 10 to 100 Hz, plotted in the lower part of Figure 1, show that this windscreen had a large transmission coefficient at frequencies below 25 Hz, even exhibiting a gain as high as 8 dB at 10 Hz, but then attenuated sound at higher frequencies. Finally, a soak test revealed that the water absorbed by the polyurethane windscreen material amounted to only 2.1 percent by weight.

Figure 2 shows a windscreen installed over a microphone mounted on a pole in the field. The windscreen has proved robust in weather conditions of all seasons and it survived Hurricane Isabel with wind gusts up to 67 mph (30 m/s).

This work was done by Allan J. Zuckerwar, Qamar A. Shams, Bradley S. Sealey, and Toby Comeaux of Langley Research Center. For further information, contact the Langley Innovative Partnerships Office at (757) 864-3521. LAR-16833-1

Broadband External-Cavity Diode Laser

This relatively simple, inexpensive device is suitable for use in survey spectroscopy.

John H. Glenn Research Center, Cleveland, Ohio

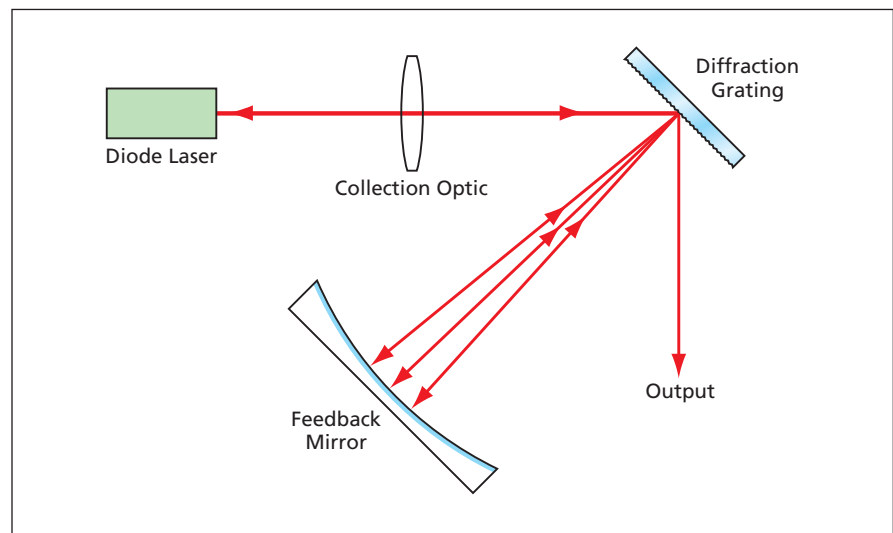
A broadband external-cavity diode laser (ECDL) has been invented for use in spectroscopic surveys preparatory to optical detection of gases. Heretofore, commercially available ECDLs have been designed, in conjunction with sophisticated tuning assemblies, for narrow-band (and, typically, single-frequency) operation, as needed for high sensitivity and high spectral resolution in some gas-detection applications. However, for preparatory spectroscopic surveys, high sensitivity and narrow-band operation are not needed; in such cases, the present broadband ECDL offers a simpler, less-expensive, more-compact alternative to a commercial narrowband ECDL.

To be precise, the output of the tunable, broadband ECDL consists of many narrow spectral peaks spaced at narrow wavelength intervals that, taken together, span a broad wavelength band. The broadband ECDL can, therefore, be likened to a light-emitting diode except that the spectrum incorporates the external-cavity mode structure. Unlike

light-emitting diodes, the ECDL offers the greater brightness, simpler fiber coupling, and superior spatial propagation properties of a laser. For example, the broadband ECDL is easily coupled into multiple-pass optical-path-length-

enhancement cells. A tunable filter — preferably, a monochromator or a spectrometer — is used to select a portion of the output spectrum.

The optical configuration of the broadband ECDL (see figure) is based



The **Feedback Mirror Is Made Curved** (in contradistinction to flat) to make it select a range of wavelengths (in contradistinction to a single wavelength).

on, but differs from, a standard configuration known in the art as that of the Littman-Metcalf design. Whereas heretofore, a flat feedback mirror would be used to select a single laser output wavelength, in the present case, a curved feedback mirror is used to select multiple wavelengths. Preferably, the feedback mirror is cylindrical or spherical and is positioned with its center of curvature at the point of diffraction (the intersection of the laser beam with the diffraction grating).

In this configuration, each wavelength component diffracted from the

grating is reflected from the mirror back to the point of diffraction. Thus, many wavelength components are simultaneously oscillating in the external cavity. The wavelength range is determined by the range of angles intercepted by the mirror; hence, the wavelength range can be adjusted by moving the mirror to a different position on the diffraction circle. The zeroth-order output of the diffraction grating is used as the laser output.

The length of the external cavity (including the mirror radius) determines the longitudinal mode spacing. It is

preferable to make this spacing smaller than the wavelength resolution of tunable filter, so that for the purpose of filtering, the ECDL spectrum can be regarded as continuous.

This work was done by Jeffrey S. Pilgrim of Southwest Sciences, Inc. for Glenn Research Center. Further information is contained in a TSP (see page 1).

Inquiries concerning rights for the commercial use of this invention should be addressed to NASA Glenn Research Center, Innovative Partnerships Office, Attn: Steve Fedor, Mail Stop 4-8, 21000 Brookpark Road, Cleveland, Ohio 44135. Refer to LEW-17486-1.

High-Efficiency Solar Cells Using Photonic-Bandgap Materials

Energy-conversion efficiencies exceeding 50 percent may be possible.

NASA's Jet Propulsion Laboratory, Pasadena, California

Solar photovoltaic cells would be designed to exploit photonic-bandgap (PBG) materials to enhance their energy-conversion efficiencies, according to a proposal. Whereas the energy-conversion efficiencies of currently available solar cells are typically less than 30 percent, it has been estimated that the energy-conversion efficiencies of the proposed cells could be about 50 percent or possibly even greater.

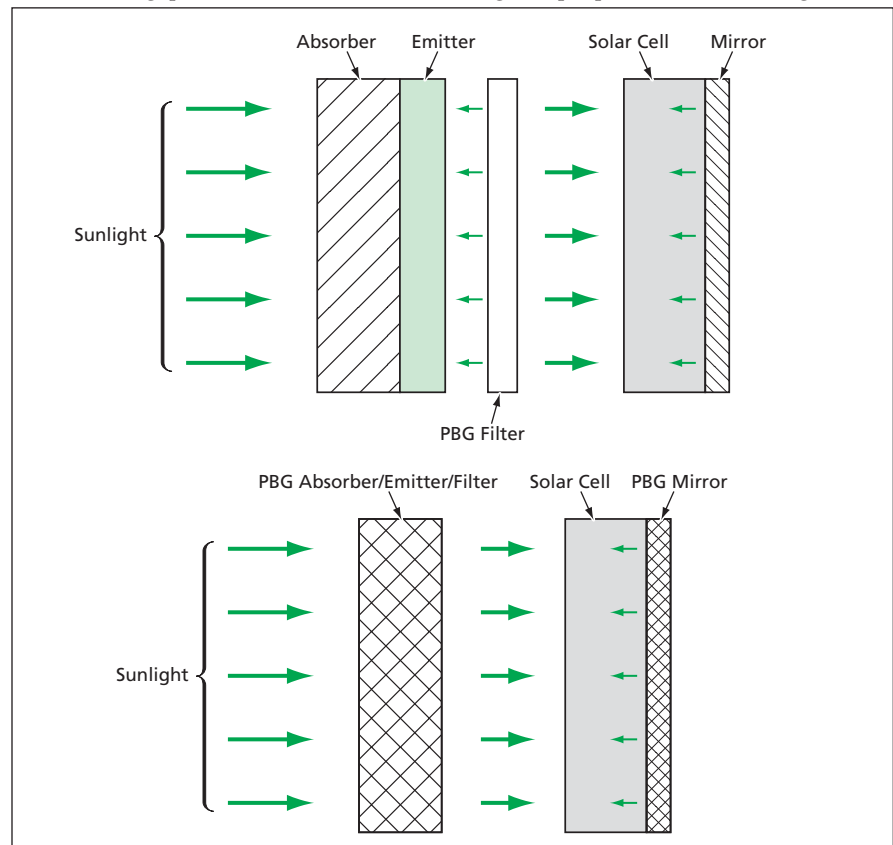
The primary source of inefficiency of a currently available solar cell is the mismatch between the narrow wavelength band associated with the semiconductor energy gap (the bandgap) and the broad wavelength band of solar radiation. This mismatch results in loss of power from both (1) long-wavelength photons, defined here as photons that do not have enough energy to excite electron-hole pairs across the bandgap, and (2) short-wavelength photons, defined here as photons that excite electron-hole pairs with energies much above the bandgap. It follows that a large increase in efficiency could be obtained if a large portion of the incident solar energy could be funneled into a narrow wavelength band corresponding to the bandgap. In the proposed approach, such funneling would be effected by use of PBG materials as intermediaries between the Sun and photovoltaic cells.

The approach involves a thermophotovoltaic principle in addition to the use of PBG materials. The basic idea is to tailor the wavelength- and direction-dependent emissivity of one or more PBG

material(s) such that as much as possible of the wavelength-mismatched portion of the incident broad-band solar power would be absorbed — the absorbed power would cause heating, and the resulting thermal radiation would be funneled into a narrow band corresponding to the bandgap of the semiconductor

material of a solar cell. Recent experiments unrelated to the development of solar cells have shown that as much as half of the thermal power could be thus re-routed into the bandgap.

The figure depicts two of many conceivable configurations for implementing the proposal. In one configuration,



PBG Materials Could Be Utilized in these and other configurations to increase the energy-conversion efficiencies of solar cells.

the incident solar radiation would be intercepted by an absorber and absorbed energy would be re-radiated by an emitter. A filter behind the emitter would allow primarily bandgap-energy photons to pass through and would reflect most other photons back into the absorber, helping to keep the absorber hot. A mirror at the rear surface of the solar cell would reflect any remaining non-bandgap-energy photons back to the absorber. The filter would be made of a PBG material: the advantage to be gained by using a PBG filter instead of a traditional optical filter is that a PBG structure could be designed to modify

the wavelength distribution of thermal radiation from a conventional black-body distribution to reduce or increase the spectral power densities at selected wavelengths.

In the other configuration, the functions of the absorber and filter would be combined in a single monolithic PBG absorber/emitter that could comprise, for example, thin absorbing layers alternating with thin non-absorbing, wavelength-selective layers. Optionally, the mirror behind the solar cell could also be made of a PBG material.

This work was done by Jonathan Dowling and Hwang Lee of Caltech for NASA's Jet

Propulsion Laboratory. *Further information is contained in a TSP (see page 1).*

In accordance with Public Law 96-517, the contractor has elected to retain title to this invention. Inquiries concerning rights for its commercial use should be addressed to:

*Innovative Technology Assets Management
JPL*

*Mail Stop 202-233
4800 Oak Grove Drive
Pasadena, CA 91109-8099
(818) 354-2240*

E-mail: iaoffice@jpl.nasa.gov

Refer to NPO-40662, volume and number of this NASA Tech Briefs issue, and the page number.



Generating Solid Models From Topographical Data

Topographical data are converted into forms useable by rapid-prototyping machines.

Goddard Space Flight Center, Greenbelt, Maryland

A method of generating solid models of terrain involves the conversion of topographical data into a form useable by a rapid-prototyping (RP) machine. The method was developed to enable the use of the RP machine to make solid models of Martian terrain from Mars Orbiter laser-altimeter topographical data. The method is equally applicable to the generation of models of the terrains of other astronomical bodies, including other planets, asteroids, and Earth.

Topographical data describe a terrain in terms of a set of three-dimensional coordinates [e.g., Cartesian (x,y,z) or polar (latitude, longitude, radius) coordinates] of points or nodes on the terrain surface. The input data for the RP machines are required to provide a three-dimensional description, not of a

single surface, but of a volume — in this case, a ground volume that underlies the terrain surface. The description is required to be in the form of triangular elements that connect the nodes of all the surfaces and that completely bound the volume, with no open areas, no overlap of triangles, and no extraneous geometric elements.

The software used in the present model-generation method was written in IDL — an advanced programming language that affords a number of tools, including subroutines that triangularize surfaces. The software creates a volume from the topographical surface data by adding sides to the edges of the terrain surface and joining the sides with a bottom surface. Each of the sides is triangularized by use of IDL subrou-

tines, and then the software searches for extraneous elements and removes them.

Topographical data are usually presented in a grid corresponding to polar coordinates, so that a model generated from such data is equivalent to a topographical map in Mercator projection. However an RP machine is fully capable of including the curvature of a planetary body in a model that it makes. Therefore, the software also offers a capability to transform the topographical data to a projection onto a surface having a curvature corresponding to that of the surface of the modeled planet.

This work was done by John W. Keller of Goddard Space Flight Center. Further information is contained in a TSP (see page 1). GSC-14897-1

Computationally Lightweight Air-Traffic-Control Simulation

This algorithm simulates ATC functions for a busy airport.

NASA's Jet Propulsion Laboratory, Pasadena, California

An algorithm for computationally lightweight simulation of automated air-traffic control (ATC) at a busy airport has been derived. The algorithm is expected to serve as the basis for development of software that would be incorporated into flight-simulator software, the ATC component of which is not yet capable of handling realistic airport loads. Software based on this algorithm could also be incorporated into other computer programs that simulate a variety of scenarios for purposes of training or amusement.

The ATC simulation problem that the algorithm is meant to solve can be summarized as follows: ATC is responsible for all aircraft that enter an arbitrarily specified hemisphere, denoted the flight-simulator bubble, that is centered at the airport. ATC must guide all the aircraft to safe landings in a sequence that is as fair as possible under the circumstances. Information about the airport that is taken into account

includes the lengths, directions, and locations of end points of runways. Information about each aircraft that is taken into account includes the current three-dimensional position and velocity, maximum and minimum speeds, and mathematical relationships among turning times and the starting and ending points of turns between specified headings. The solution generated by the algorithm must be a set of instructions to the aircraft that enable all aircraft to land without violating any constraints.

The algorithm consists of four components denoted the controller, the plan, the vector generator, and the constraint verifier. The controller is event-driven and relatively simple: It responds to any of three events, as follows:

1. An aircraft enters the bubble. The controller tries all vector options in a shortest-path-first order, checking each by use of the constraint verifier. When a solution is found, the con-

troller issues instructions to the appropriate pilots.

2. An aircraft leaves the bubble. The controller removes the aircraft from the plan.

3. An aircraft changes location as prescribed by the plan. The controller causes the plan to be updated with the new location and time of arrival of the aircraft at the location. If necessary, it gives instructions to the appropriate pilot.

Thus, the controller is the input/output interface for the ATC.

The plan is a data structure that is used to verify current and hypothetical routing for each aircraft. The plan consists of a simple temporal network (STN) augmented by labeling of time points with identities of aircraft and of other time points with which overlaps must be prevented. The approach followed by an aircraft is represented as a directed path in the STN. Inasmuch as each aircraft has its own unique path,

the overlap labels are used to enforce the fundamental constraint that no two aircraft may be in the same place at the same time. If two time points overlap in space, then it is necessary to ensure that they do not overlap in time. This is done by introducing temporal constraints. Operations on the plan include insertion of an aircraft, deletion of an aircraft, and updating of the position and time of an aircraft. An aircraft is inserted into the plan by inserting its approach.

The approach generator generates a series of time points and temporal constraints that represent a hypothetical approach for an aircraft. It also generates the information for the overlaps for each time point of the plan. The approach

generator includes a vector generator that iterates over options from most preferred (a full-procedure approach) to least preferred (one or more turns in a holding pattern, ending in a direct approach). Once a vector is generated, it must be verified as described in the next paragraph. If verified, it is incorporated into the plan.

The constraint verifier checks a plan and introduces temporal constraints where necessary to maintain veracity. The constraint verifier identifies time points that lack temporal ordering between themselves and members of their overlap set. It then incrementally inserts ordering constraints and verifies that each constraint is possible using temporal propagation. It can preferentially

schedule new points either before or after pre-existing points, according to the preferences of the designers of the ATC system. Once a verified plan is found, the verifier returns "true." If a verified plan cannot be found, the verifier returns "false" and removes any extraneous temporal constraints it inserted.

*This work was done by Russell Knight of Caltech for **NASA's Jet Propulsion Laboratory**. Further information is contained in a TSP (see page 1).*

The software used in this innovation is available for commercial licensing. Please contact Karina Edmonds of the California Institute of Technology at (818) 393-2827. Refer to NPO-40445.



Spool Valve for Switching Air Flows Between Two Beds

U.S. Patent 6,142,151 describes a dual-bed ventilation system for a space suit, with emphasis on a multiport spool valve that switches air flows between two chemical beds that adsorb carbon dioxide and water vapor. The valve is used to alternately make the air flow through one bed while exposing the other bed to the outer-space environment to regenerate that bed through vacuum desorption of CO₂ and H₂O. Oxygen flowing from a supply tank is routed through a pair of periodically switched solenoid valves to drive the spool valve in a reciprocating motion. The spool valve equalizes the pressures of air in the beds and the volumes of air flowing into and out of the beds during the alternations between the adsorption and desorption phases, in such a manner that the volume of air that must be vented to outer space is half of what it would be in the absence of pressure equalization. Oxygen that has been used to actuate the spool valve in its reciprocating motion is released into the ventilation loop to replenish air lost to vacuum during the previous desorption phase of the operating cycle.

This work was done by W. Clark Dean of United Technologies Corp. for Johnson Space Center.

Title to this invention, covered by U.S. Patent No. 6,142,151 has been waived under the provisions of the National Aeronautics and Space Act {42 U.S.C. 2457 (f)}. Inquiries concerning licenses for its commercial development should be addressed to:

*Hamilton Sundstrand
Space Systems International, Inc.
One Hamilton Road
Windsor Locks, CT 06096-1010
Phone No.: (860) 654-6000*

Refer to MSC-23667, volume and number of this NASA Tech Briefs issue, and the page number.

Partial Model of Insulator/Insulator Contact Charging

Two papers present a two-phase equilibrium model that partly explains insulator/insulator contact charging. In this model, a vapor of ions within a gas is in equilibrium with a submonolayer

of ions of the same species that have been adsorbed on the surface of an insulator. The surface is modeled as having localized states, each with a certain energy of adsorption for an ion. In an earlier version of the model described in the first paper, the ions do not interact with each other. Using the grand canonical ensemble, the chemical potentials of both vapor and adsorbed phases are derived and equated to determine the vapor pressure. If a charge is assigned to the vapor particles (in particular, if single ionization is assumed), then the surface charge density associated with adsorbed ions can be calculated as a function of pressure. In a later version of the model presented in the second paper, the submodel of the vapor phase is extended to include electrostatic interactions between vapor ions and adsorbed ones as well as the screening effect, at a given distance from the surface, of ions closer to the surface. Theoretical values of this model closely match preliminary experimental data on the discharge of insulators as a function of pressure.

*This work was done by Michael Hogue, C. I. Calle, and C. R. Buhler of Kennedy Space Center and E. R. Mucciolo of the University of Central Florida. Further information is contained in a TSP (see page 1).
KSC-12722*

Asymmetric Electrostatic Radiation Shielding for Spacecraft

A paper describes the types, sources, and adverse effects of energetic-particle radiation in interplanetary space, and explores a concept of using asymmetric electrostatic shielding to reduce the amount of such radiation impinging on spacecraft. Typically, such shielding would include a system of multiple inflatable, electrically conductive spheres deployed in clusters in the vicinity of a spacecraft on lightweight structures that would maintain the spheres in a predetermined multipole geometry. High-voltage generators would maintain the spheres at potential differences chosen in conjunction with the multipole geometry so that the resulting multipole field would gradually divert approaching energetic atomic nuclei from a central region occupied by the

spacecraft. The spheres nearest the center would be the most positive, so as to repel the positively charged impinging nuclei from the center. At the same time, the monopole potential of the overall spacecraft-and-shielding system would be made negative so as to repel thermal electrons. The paper presents results of computational simulations of energetic-particle trajectories and shield efficiency for a trial system of 21 spheres arranged in three clusters in an overall linear quadrupole configuration. Further development would be necessary to make this shielding concept practical.

This work was done by Philip T. Metzger and Robert C. Youngquist of Kennedy Space Center and John E. Lane of ASRC Aerospace. Further information is contained in a TSP (see page 1).

This invention is owned by NASA, and a patent application has been filed. Inquiries concerning nonexclusive or exclusive license for its commercial development should be addressed to the Kennedy Innovative Partnerships Office at (321) 867-8130. Refer to KSC-12624.

Reusable Hybrid Propellant Modules for Outer-Space Transport

A report summarizes the concept of reusable hybrid propellant modules (HPMs), which would be used in outer space for long-term cryogenic storage of liquefied spacecraft-propellant gases, including for example, oxygen and hydrogen for combustion-based chemical rocket engines and xenon for electric thrusters. The HPM concept would provide the fundamental building block for an efficient, reusable in-space transportation system for both crewed and uncrewed missions. Each HPM would be equipped to implement an advanced zero-boil-off method of managing cryogenic fluids, and would include a fluid-transfer interface comprising standardized fittings that would be compatible with fittings on all supply facilities and on spacecraft to be supplied. The HPM, combined with a chemical or electric orbital transfer spacecraft, would provide an integrated propulsion system. HPMs would supply chemical propellant for time-critical transfers such as crewed missions, and utilize the more efficient electric-propulsion transfer vehicles to trans-

port filled HPMS to the destinations and to return empty HPMS back to near-Earth orbits or other intermediate locations for replenishment and reuse. The HPM prepositioned using electric propulsion would provide the chemical propellant for the crew's return trip in a much more efficient manner than a chemical-only approach. The propellants to fill the HPMS would be delivered from the Earth or

other initial supply locations to the intermediate locations by use of automated, compatible spacecraft designed specifically for that purpose. Additionally, multiple HPMS could be aggregated and positioned in orbits and on planets, moons, and asteroids to supply fluids to orbiting and interplanetary spacecraft.

*This work was done by Daniel D. Mazanek of **Langley Research Center** and John C.*

Mankins of the NASA Headquarters Advanced Projects Office. Further information is contained in a TSP (see page 1).

This invention is owned by NASA, and a patent application has been filed. Inquiries concerning nonexclusive or exclusive license for its commercial development should be addressed to the Patent Counsel, Langley Research Center, at (757) 864-3521. Refer to LAR-16237.



National Aeronautics and
Space Administration